



Research on global trajectory planning for UAV based on the information interaction and aging mechanism Wolfpack algorithm

Jinyu Zhang ^{a,b} , Xin Ning ^{a,b}, Shichao Ma ^{a,b,*} , Rugang Tang ^{a,c}

^a Northwestern Polytechnical University, School of Astronautics, Xi'an 710072, China

^b National Key Laboratory of Aerospace Flight Dynamics, Xi'an 710072, China

^c Hong Kong Polytechnic University, Department of Aeronautical and Aviation Engineering, Hong Kong 999077, China

ARTICLE INFO

Keywords:

Wolfpack algorithm
Unmanned aerial vehicle
Global trajectory planning

ABSTRACT

The planning of trajectories for multi-unmanned aerial vehicles (UAVs) has been a topic of intensive research in both military and civilian contexts. It is a crucial aspect of the overall intelligence capabilities of UAV formation systems. In order to enhance the capability of multi-UAVs autonomous trajectory planning and to facilitate attainment of optimal paths in mountainous environments, this paper proposes an information interaction and aging mechanism Wolfpack Algorithm (IIAM-WPA). Firstly, a mission environment model is established using digital elevation modelling technology to simulate the real mountainous environment. Secondly, a trajectory planning model is established by comprehensively considering the terrain, threats and formation security factors. Meanwhile, in order to comprehensively evaluate the planning results, a new composite objective function is proposed. The proposed IIAM-WPA method is finally employed to identify the optimal paths for multiple UAVs. The key improvements to the method are as follows: the initialization effect is enhanced by the Chebyshev chaotic mapping in initialization phase, thereby accelerating the convergence of the population. Furthermore, the aging mechanism of wolves is incorporated into the model to enhance the efficiency of wolf search. Meanwhile, communication between populations is augmented during the encirclement phase, which serves to enhance population diversity. Finally, a selective mutation mechanism is introduced to rescue the population from the local optimum trap. In order to ascertain the effectiveness of the proposed algorithm, the simulation results of UAV trajectory planning under different mission scenarios are presented and compared with various optimization techniques. The simulation results demonstrate that the maximum improvement rate of the proposed algorithm is 96.73% and 4.2% in single UAV and multi-UAV planning tasks, respectively. This further verifies the planning accuracy and efficiency of the IIAM-WPA method and effectively proves the effectiveness of the method in solving UAV trajectory planning problems.

1. Introduction

In recent years, UAVs have been employed extensively in both civilian and military contexts, due to a number of factors, including their high mobility, low cost, good safety record and ability to operate effectively in challenging environments, such as disaster relief, logistics transportation, reconnaissance and detection, tracking and positioning and other tasks (Chen et al., 2021; Xing & Johnson, 2023; Yao et al., 2023; Ning et al., 2024). Among them, flight path planning is the core aspect of UAV task execution, with the quality of this planning directly influencing the UAV's ability to complete its assigned tasks. In this context, the efficacy of flight path planning is a crucial determinant of

the autonomous capabilities of the UAV (Cabeira et al., 2019). Nevertheless, the accelerated development of unmanned technologies and the complexity of missions present considerable challenges to the path planning capabilities of UAVs, particularly in the context of enemy radar, mountainous terrain, and no-fly zones.

In order to address this issue, a significant number of research scholars have dedicated their efforts to the investigation of UAV trajectory planning methods in complex environments, with the objective of enhancing mission completion rates and safety (Fu et al., 2022; Kyriakakis et al., 2022; Xu et al., 2022; Fuertes et al., 2023; Liu et al., 2023a). In the past decades, many methods and algorithms have been developed, which in this paper are classified into four categories

* Corresponding author at: Northwestern Polytechnical University, School of Astronautics, Xi'an 710072, China.

E-mail address: shichaoma@nwpu.edu.cn (S. Ma).

Methodology Classification	2D extension method	Sampling-based search method	Bio-inspired method	Machine learning method
Common Algorithms	A* algorithm Dijkstra method depth-first method	RRT PRM	PSO WPA DE	reinforcement learning deep learning
Advantages	Simple principle easy to implement	Simple Principle Suitable for high dimensions	Fast convergence Parallelism	Self-learning Suitable for high dimensions
Disadvantages	Inefficiency in solving complex tasks	Dependence on sample quality non-optimal solution	Declining search capability Local optimality phenomenon	Dependent on parameter settings Long-term training

Fig. 1. Advantages and disadvantages of the four types of methods.

according to their characteristics, as elaborated upon in the following sections.

The first is the 2D extension method, which conducts the search by abstracting the task scenario into a grid topology graph. This category of methodologies encompasses algorithms such as A-star algorithm (Zhang et al., 2023; Ha, 2024), Dijkstra method (Campo et al., 2020; Xu et al., 2020; Wang et al., 2022a), Depth-first method (Rouillon et al., 2006; Wu et al., 2023), and others. While this approach is relatively straightforward in principle, the search cost and solving difficulty will increase exponentially with the complexity of the task scenario. In order to enhance the efficiency of the algorithm solution, numerous researchers have made contributions to the field. For instance, Zhang incorporated the radar threat as a cost into the heuristic function and employed a variable step search strategy to enhance the search efficiency, thereby improving the planning efficiency (Zhang et al., 2023). Similarly, Wang augmented the accuracy of the planning by utilizing the matrix alignment method to reduce the search complexity and implementing forward search and backward navigation strategies to improve the search efficiency (Wang et al., 2022a). Despite the numerous enhancements that have been made to these methodologies, it remains challenging to ensure their computational efficiency in addressing complex problems. Consequently, the method is primarily appropriate for path planning in straightforward scenarios.

The second is the sampling-based search method. These methods encompass a range of algorithms, including RRT (Chen et al., 2018; Jeong et al., 2019; Kang et al., 2024) and PRM (Wang et al., 2015; Liu et al., 2023b), among others. In comparison with the 2D expansion method, this type of algorithm does not necessitate the specific modeling of the task scenario and can be utilized to solve path planning problems in complex environments. However, this method is characterized by strong randomness, resulting in paths obtained from each solution being distinct. Additionally, it generates a greater number of redundant nodes, and the planning results are contingent on the quality of the sampling points, which complicates the assurance of optimality and the stability is suboptimal. Addressing these existing issues, Kang enhanced the efficiency of path planning by adjusting the expansion direction of a random tree and setting the dynamic step size (Kang et al., 2024); Wu proposed a stochastic steering extension strategy with the objective of enhancing planning capability and efficiency in narrow regions (Wu et al., 2021). Nevertheless, current research endeavors continue to encounter challenges in addressing the issue of excessive randomness in sampling-based methods, rendering them ill-suited for

scenarios where accuracy is paramount.

Also included is the bio-inspired Algorithm, an intelligent algorithm developed by studying the behavior patterns of organisms in nature, aiming to simulate their survival and cooperation mechanisms, thereby increasing the efficiency of the algorithm. The method include algorithms such as particle swarm algorithm (PSO) (Zhang et al., 2010; Song et al., 2023; Yildiz et al., 2024), and the wolfpack algorithm (WPA) (Wu et al., 2020; Xiu-wu et al., 2020; She et al., 2023), Differential evolutionary algorithms (DE) (Wu et al., 2018; Wang & Ma, 2023), and so on. This method is robust, scalable and simple in structure, and has been widely used to solve path planning problems in recent years. Nevertheless, the algorithm is vulnerable to a phenomenon termed premature maturation, which occurs when the local search capability diminishes in the late stages of computation, resulting in local optimum solutions. Addressing these issues has prompted numerous researchers to conduct studies in this area. For instance, Yildiz have proposed a novel swarm topology, integrating the strengths of PSO and the enhanced RRT algorithm, to enhance the precision of planning outcomes. Nevertheless, this approach necessitates a more protracted optimization process (Yildiz et al., 2024). Meanwhile, Wang propose a segmented evolution strategy, which can enhance local optimality seeking while preserving the value of the main body of the population. However, excessive segmentation can lead to an increase in algorithmic complexity and a reduction in efficiency (Wang & Ma, 2023). Therefore, it is imperative that the efficiency and accuracy of computation are considered in their totality when employing the bionic algorithm.

Furthermore, the subject matter incorporates machine learning methodologies, which encompass such techniques as reinforcement learning (Zhou et al., 2021; Wang et al., 2022b; Yu & Luo, 2023; Lee & Ahn, 2024) and deep learning (Li et al., 2020; Krishnan et al., 2021; Li et al., 2024; Lin et al., 2024). This method has the capacity for autonomous learning, with the capability of continuously enhancing its own planning capabilities through the training of the network, thereby leading to improved planning outcomes. The utilization of the trained network facilitates the expeditious attainment of optimal planning results. Nevertheless, it is imperative to allocate a substantial amount of time to the training phase to ensure the efficacy of the results. Additionally, the portability of this method is suboptimal, making it challenging to ascertain the advantages and disadvantages of the planning results when the task scenario undergoes significant alterations. The advantages and disadvantages of the aforementioned methods are outlined in Fig. 1.

Among the above algorithms, WPA is a bio-inspired algorithm modeled after the predation behavior of wolves in nature. It has been shown to exhibit superior global convergence and computational robustness, making it an effective approach for solving high-dimensional and multi-modal optimization problems. As a result, it has garnered significant attention from researchers, leading to certain advancements in this area. Among them, Wu improved the head wolf update rule and used inversion as well as movement operators to improve the computational efficiency of the algorithm (Wu et al., 2020); Xiu improved the movement of wolves and siege step to avoid the algorithm from falling into local optimum prematurely (Xiu-wu et al., 2020); A binary wolf pack algorithm was proposed in the literature (Wu & Xiao, 2020) to improve the algorithm's ability to adapt to the environment through a new population update strategy; Peng designed a centralized decision-making coalition mechanism, which combines individual competition with overall coordination, effectively solving the problem of task allocation for multiple UAVs (Peng et al., 2024); and Shao used an improved wolfpack algorithm to obtain an ideal tracking path and tracked the trajectory based on the backstepping method, which improved the quality of the trajectory as well as the stability of the trajectory tracking system (Shao et al., 2023).

From the above literature, it can be seen that many researchers have meticulously studied WPA and achieved certain results and progress. However, there are fewer studies using WPA to solve the multi-UAV trajectory planning problem, and there are also still some limitations and deficiencies. The most salient of these limitations pertains to the WPA's paucity in information transfer, rendering it entirely dependent on the head wolf's leadership. This dependency can result in the over-concentration of wolves on subsequent positions, potentially leading to stagnant path searches. Additionally, the WPA exhibits premature maturation, which complicates the assurance of optimal directional movement. Furthermore, scout wolves search for prey in fixed and parallel directions, which poses a challenge to maintain population diversity and increases the risk of local optimization. Consequently, there is an urgent need for an accurate, efficient and versatile UAV trajectory planning method.

Based on the above limitations, in order to ensure that UAV can perform their missions safely and efficiently in complex environments, this paper proposes an information interaction and aging mechanism Wolfpack Algorithm (IIAM-WPA). The following enhancements have been introduced: First, an improved Chebyshev mapping method is applied at the initial stage of the wolf population to increase dispersion and enhance search capabilities. Second, a “coarse-to-fine” strategy is implemented during the wolf detection phase, with the introduction of an age factor to improve search efficiency and avoid premature convergence to local optima. Subsequently, by mimicking the natural predation process, the quality of information interaction with high-performing individuals during the siege phase is enhanced, thereby reducing the risk of losing valuable information. Finally, an improved reverse Gaussian-Cauchy variation method is proposed to increase the diversity of wolf populations by applying perturbations, thereby preventing the algorithm from becoming trapped in local optima.

The main contributions of this paper can be briefly summarized as follows:

- (1) This paper presents a novel global path planning method for multi-UAV tracking missions. The method employs a wolf pack ageing mechanism that effectively avoids local optimal risk and improves the accuracy of the planning results by eliminating old individuals in the population.

- (2) The proposed hierarchical composite objective function considers a multitude of factors pertinent to the UAV trajectory planning task, adjusting them according to their respective degrees of influence. This approach simplifies the inherently complex trajectory planning problem into an optimisation problem, thereby reducing the difficulty of solving the problem in complex task scenarios.
- (3) This paper presents a novel approach to target tracking based on an adaptive strategy that utilises population information, coupled with the siege mechanism inherent to the wolf pack algorithm. This strategy enables real-time adjustments to the tracking direction, effectively addressing the challenge of premature maturity of the population in multi-polar environments.
- (4) Through the simulation and comparison of multiple sophisticated algorithms in a variety of intricate contexts, the proposed algorithm has reached an exceptional level of advancement. It is capable of effectively circumventing local optimal pitfalls and rapidly attaining a superior UAV flight path.

The rest of the paper is organized as follows. In Section 2 a trajectory planning model for UAV is established, including environmental threat modelling, planning constraints, and objective indicator functions. Section 3 briefly introduces the WPA and analyses its deficiencies, and proposes the specific implementation process of IIAM-WPA for the trajectory planning method. In Section 4, simulations are carried out in a variety of mission scenarios and compared with other planning algorithms to verify the effectiveness of the proposed algorithm. Finally, the paper is summarized in Section 5 and main conclusions are given.

2. UAV trajectory planning model

In the context of UAV cooperative missions, trajectory planning represents a pivotal technology, it is used to determine the feasibility and efficiency with which UAVs can complete their assigned tasks (Xie et al., 2023; Wan et al., 2024). Factors such as the mission environment, enemy threats, and UAV inter-flight safety must be considered during the planning process, so a comprehensive assessment of all relevant factors is required to ensure that the outcome of the plan is reasonable. This paper presents a decoupling and simplification of the complex task, abstracting it into a multi-objective optimization problem. Furthermore, it introduces a novel composite assessment index, which enhances the reliability of the assessment while reducing the complexity of the solution. In order to ensure the precision of the optimization procedure, this chapter will present a comprehensive account of the four constituent elements of the UAV motion model, the environmental model, the objective function, and the constraints. The particulars of these elements will be discussed in subsequent sections.

2.1. UAV motion model

In order to accurately describe the UAV trajectory planning process, the UAV model is presented in this section. In this study, the UAV is considered as a particle with attitude information while flying in 3D space, which ignores the effect of factors such as air resistance. The following simplified UAV motion model is presented:

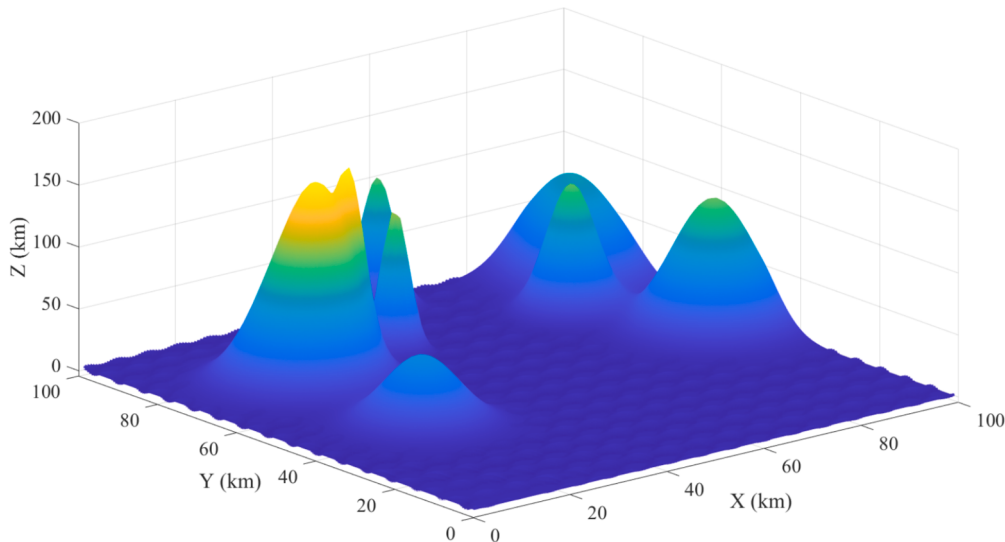


Fig. 2. DEM mission terrain.

$$\begin{aligned}
 \dot{x} &= u \cdot \cos\theta \cos\psi + v(\sin\phi \sin\theta \cos\psi - \cos\phi \sin\psi) + w(\cos\phi \sin\theta \cos\psi + \sin\phi \sin\psi) \\
 \dot{y} &= u \cdot \cos\theta \sin\psi + v(\sin\phi \sin\theta \sin\psi + \cos\phi \cos\psi) + w(\cos\phi \sin\theta \sin\psi - \sin\phi \cos\psi) \\
 \dot{z} &= -u \sin\theta + v \sin\phi \cos\theta + w \cos\phi \cos\theta \\
 \dot{\phi} &= p + q \sin\phi \tan\theta + r \cos\phi \tan\theta \\
 \dot{\theta} &= q \cos\phi - r \sin\phi \\
 \dot{\psi} &= q \sin\phi / \cos\theta + r \cos\phi / \cos\theta
 \end{aligned} \tag{1}$$

Where (x, y, z) represents the positional coordinates of the UAV; (u, v, w) is the velocity parameter of the UAV; (θ, ψ, ϕ) is the pitch angle, yaw angle and roll angle of the UAV during flight; (p, q, r) is the angular velocity of the UAV during its pitch, yaw, and roll, respectively.

During UAV flight, its state is usually described in two coordinate systems, the geocentric coordinate system (WGS84) and the fuselage coordinate system, and in order to solve the parameters of the UAV, a transformation between the two coordinate systems is required, and the coordinate transformation matrix is as follows:

$$R_{b2n} = \begin{bmatrix} \cos\theta \cos\psi & \cos\theta \sin\psi & -\sin\theta \\ \sin\phi \sin\theta \cos\psi - \cos\phi \sin\psi & \sin\phi \sin\theta \sin\psi + \cos\phi \cos\psi & \sin\phi \cos\theta \\ \cos\phi \sin\theta \cos\psi + \sin\phi \sin\psi & \cos\phi \sin\theta \sin\psi - \sin\phi \cos\psi & \cos\phi \cos\theta \end{bmatrix} \tag{2}$$

By using the above equation, we can get the position parameters of the UAV in the geocentric coordinate system, which facilitates the solution of the parameters in the planning process.

2.2. Mission environment model

In order to ensure the effectiveness of the planning trajectory, this paper adopts a digital elevation model (DEM) to simulate the irregular terrain of the mountainous mission environment, which is decomposed into the original terrain and the threatening terrain. The mathematical model of the original terrain can be described as follows:

$$\begin{aligned}
 z_1(x, y) = & \sin(y + a) + b \cdot \sin(x) + c \cdot \cos(d \cdot \sqrt{x^2 + y^2}) + e \cdot \cos(y) \\
 & + f \cdot \sin(g \cdot \sqrt{x^2 + y^2})
 \end{aligned} \tag{3}$$

Where x, y represent the coordinates of the projected points of the model; z_1 represents the height of the corresponding points of the base terrain; and the rest of $a \sim g$ are constant coefficients, which are related

to the ups and downs of the model map.

The higher peak terrain can be represented by the following function:

$$z_2(x, y) = \sum_{i=1}^n h_i * \exp\left(\frac{(x - x_i)^2}{x_{si}} + \frac{(y - y_i)^2}{y_{si}}\right) \tag{4}$$

Where (x_i, y_i) is the center coordinate of the i th mountain; x_{si}, y_{si} represent the attenuation degree of the i th peak in the x, y direction; h_i represents the slope of the peak; n is the total number of peaks.

Fig. 2 shows a random elevation map generated using the digital elevation model.

2.3. Trajectory planning objective function

The planning of multi-UAV trajectories represents a complex multi-objective optimisation problem, necessitating the simultaneous consideration of a multitude of factors. In order to address this challenge, this paper puts forth a novel composite objective function that integrates a range of factors, including range, collision loss, and trajectory safety, and categorizes them according to their respective importance. The objective function utilized for planning is as follows:

$$F = (f_L \cdot e^{\varphi_1 f_E} \cdot e^{\varphi_2 f_C} \cdot \varphi_3 f_R + e^{\varphi_4 f_S}) - f_B \tag{5}$$

In this context, the objective function (F) of UAV trajectory planning is represented by a set of indicators ($f_L \sim f_B$), which encompasses terrain collision indicator, UAV collision indicator, planning path smoothness indicator, threat indicator, and optimal path indicator. The degree of influence of these different indicators on the resulting trajectory planning is represented by $\varphi_1 \sim \varphi_4$. In this paper, the weights will be set according to the type of parameters and the degree of importance. For instance, the parameters pertaining to collisions and threats exert a

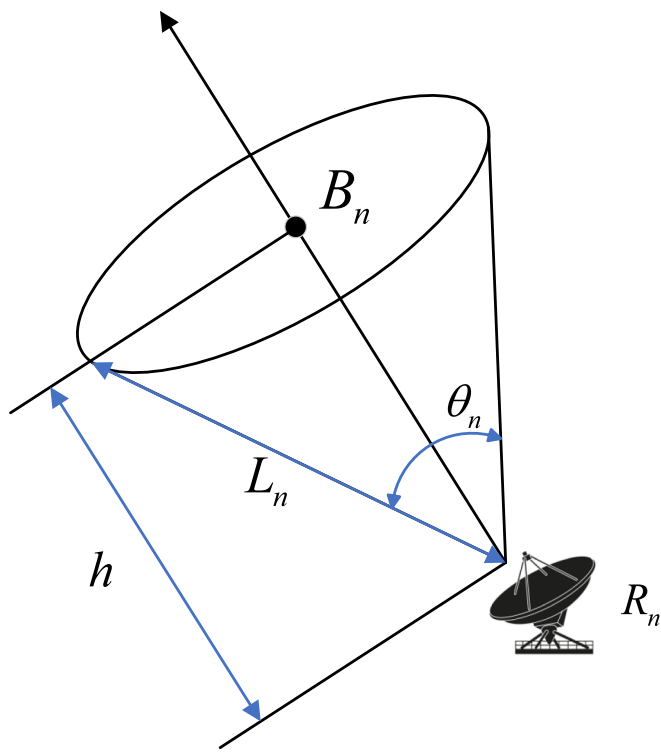


Fig. 3. Radar detection model.

greater influence on the successful completion of the task; thus, $\varphi_1 \sim \varphi_3$ is assigned a larger value. Conversely, the degree of path smoothness exerts a comparatively insignificant influence on task completion and is consequently assigned a lower value.

The specifics of each parameter in the objective function are as follows.

(1) Flight range indicator

$$f_L = \sum_{i=1}^{k-1} \sqrt{(x_{i+1} - x_i)^2 + (y_{i+1} - y_i)^2 + (z_{i+1} - z_i)^2} \quad (6)$$

Where f_L is the planning flight range cost and (x, y, z) is the position information of the planning track point.

(2) Topographic collision indicator

$$f_E = \begin{cases} 0 & \text{path}(x, y) - S(x, y) \geq h \\ \alpha \text{path}(x, y) - S(x, y) & < h \end{cases} \quad (7)$$

Where f_E is the terrain collision cost; α is the terrain collision penalty coefficient; S is the terrain obstacle height; and path is the UAV flight height.

(3) Inter-UAV collision indicator

$$f_C = \begin{cases} 0, & R_{\text{safe}} \geq \sqrt{(x_{1i} - x_{2i})^2 + (y_{1i} - y_{2i})^2 + (z_{1i} - z_{2i})^2} \\ \gamma, & R_{\text{safe}} < \sqrt{(x_{1i} - x_{2i})^2 + (y_{1i} - y_{2i})^2 + (z_{1i} - z_{2i})^2} \end{cases} \quad (8)$$

Where f_C is the UAV inter-copter collision cost; γ is the UAV collision penalty coefficient; R_{safe} is the UAV inter-copter safety distance.

(4) Track smoothing indicator

$$f_S = \sum_{i=1}^{m-1} \mu_0 \cdot (1 + \cos\theta) \quad (9)$$

Where f_S is the planning path smoothing index; μ_0 is the smoothing gain coefficient; and θ is the angle between the planning track segments.

(5) Threat indicator

$$f_R = \prod_{i=1}^k \prod_{j=1}^l D_R^i D_L^j \quad (10)$$

Where f_R is the threat cost, in this paper, the threat cost is divided into the enemy radar detection area and the dangerous no-fly area, which are denoted by D_R and D_L , respectively.

In order to simulate the radar work scene, a cone model is used to simulate the detection range of radar. Fig. 3 illustrates the radar detection model.

$$D_R = \begin{cases} 1, & U_i \not\subset R_n \\ \lambda \cdot \left(\frac{L_n}{dis_{i,k}} \right)^4, & U_i \subset R_n \end{cases} \quad (11)$$

Where D_R is the enemy radar detection area; $dis_{i,k}$ represents the distance between the UAV and the radar detection center; λ is the radar detection penalty factor; L_n represents the furthest distance from the center in the radar detection area; and R_n represents the radar detection area.

In this section, two forms of no-fly zones are considered, namely airborne hazardous zones and ground hazardous zones, which are represented by spherical and cylindrical models, and the formula is expressed as follows:

$$D_{L1} = \begin{cases} 1, & dis_{i,k} > R_i \\ \beta, & dis_{i,k} \leq R_i \end{cases} \quad (12)$$

Where R_s and $dis_{i,k}$ denote the radius of the i th spherical no-fly zone and the distance of the UAV from the center of the sphere, respectively, and β is the penalty coefficient of the no-fly zone.

$$D_{L2} = \begin{cases} 1, & z - z_i > 0 \text{ and } \sqrt{(x - x_i)^2 + (y - y_i)^2} > R_i, \\ \beta, & \text{else.} \end{cases} \quad (13)$$

Where $(x_i, y_i), z_i, R_i$ represent the center, height and radius of the i th cylindrical no-fly zone, respectively.

(6) Optimum path indicator

$$f_B = \sqrt{(x_{\text{goal}} - x_{\text{start}})^2 + (y_{\text{goal}} - y_{\text{start}})^2 + (z_{\text{goal}} - z_{\text{start}})^2} \quad (14)$$

Where f_B represents the theoretical shortest trajectory length, defined as the length of the straight line connecting the starting point to the ending point.

2.4. Restrictive condition

In order to ensure the security of the UAV when performing the mission, it is essential to take into account the relevant constraints during the planning phase. This paper classifies the necessary constraints into three principal categories: the UAV's performance constraints, the Mission environmental constraints, and the collaborative constraints.

(1) UAV performance constraints.

a) Speed constraint.

During the flight of the UAV, due to the limitation of its own physical properties, its flight speed should be kept within a certain range, and the flight speed constraint as the following equation:

$$v_{\min} \leq v \leq v_{\max} \quad (15)$$

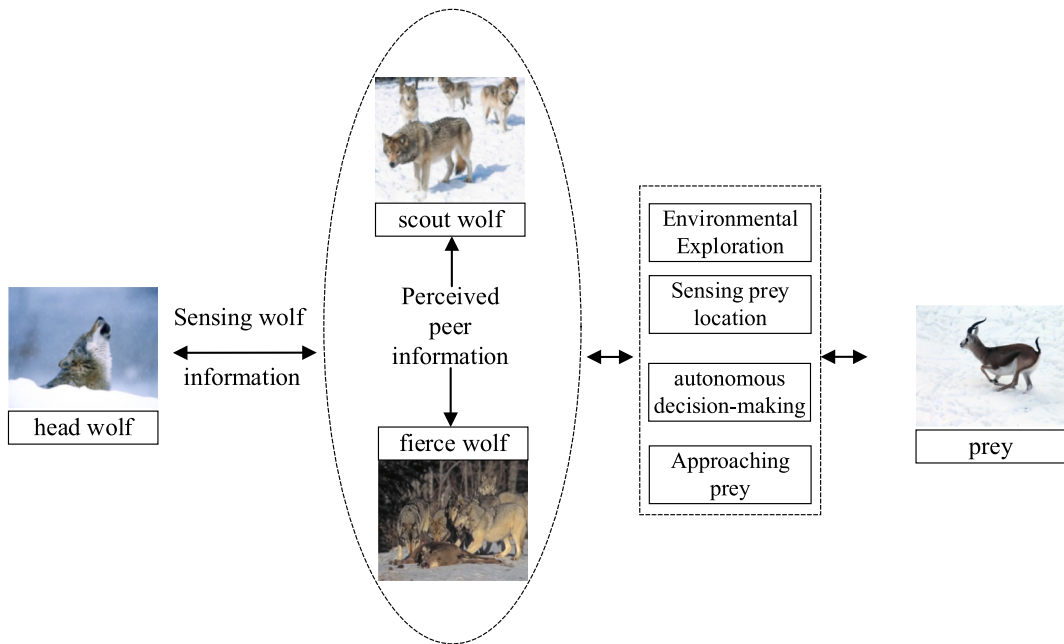


Fig. 4. Schematic of the WPA mechanism.

Where v represents the speed of the UAV during the mission; v_{\min}, v_{\max} are the minimum and maximum flight speed of the UAV.

b) Maximum turning angle constraint.

To evade enemy detection and avoid collisions, UAV must adjust its flight trajectory. It is imperative that the angle of turn is less than the maximum angle of turn, which can be expressed as follows:

$$\frac{P_i^T \cdot P_{i+1}}{|P_i| |P_{i+1}|} \leq \cos \gamma_{\max} \quad (16)$$

Where P_i is the flight path segment vector; $P_i = (x_i - x_{i-1}, y_i - y_{i-1}, z_i - z_{i-1})^T$; γ_{\max} is the maximum turning angle.

c) Maximum range constraint.

In actual flight the UAV have a limited range due to the fuel constraint, so each UAV's flight range cannot exceed its maximum flight distance. The range constraint is expressed as:

$$L_i < L_i^{\max} (\forall \text{UAV}_i \in \text{UAV}) \quad (17)$$

Where L_i is the flight range of UAV and L_i^{\max} is the maximum flight range of UAV.

d) Maximum climb/dive angle constraint.

To avoid stalling of the UAV, the climb/dive angle during flight should not be too large and the constraint can be written as:

$$\theta_i = \arctan \left(\frac{|z_{i+1} - z_i|}{\sqrt{(x_{i+1} - x_i)^2 + (y_{i+1} - y_i)^2}} \right) \quad (18)$$

$$\theta_i < \theta_{\max}$$

Where θ_i is the climb/dive angle of the UAV during flight; θ_{\max} is the maximum climb/dive angle to ensure normal UAV flight.

e) Maximum roll angle constraint.

In order to ensure the flight safety of the UAV and to achieve an effective turn, it is imperative that the roll angle should not be excessively large during the flight process, the constraint can be written as:

$$\begin{aligned} \phi_i &= \arctan \left(\frac{v_i^2}{gR} \right) \\ \phi_i &< \phi_{\max} \end{aligned} \quad (19)$$

Where ϕ_i is the roll angle of the UAV during flight; ϕ_{\max} is the maximum roll angle to ensure normal UAV flight; v_i is the UAV flight speed, g is the gravitational acceleration, and R is the UAV turning radius.

(2) Mission environmental constraints.

a) Boundary constraint.

To ensure effective mission execution, it needs to be ensured that the UAV is within the specified mission area and the following equation shows the boundary constraints.

$$\begin{cases} x_{\min} \leq x \leq x_{\max} \\ y_{\min} \leq y \leq y_{\max} \\ z_{\min} \leq z \leq z_{\max} \end{cases} \quad (20)$$

Where (x, y, z) denotes the position of the UAV; $x_{\min} \sim z_{\max}$ is the UAV flyable area boundary value.

b) Topographic constraint.

The UAV needs to avoid the spatial terrain during flight, and if the flight path intersects with the terrain, the UAV is considered to have crashed. The terrain constraints can be expressed as:

$$r_i \notin T_B \quad (21)$$

Where r_i is the planned path of UAV and T_B is the terrain obstacle area.

(3) Cooperative constraint.

Multi-UAV cooperative missions require the consideration of relevant synergy constraints in addition to the constraints described above. This paper categorizes the constraint into two types: spatial synergy and

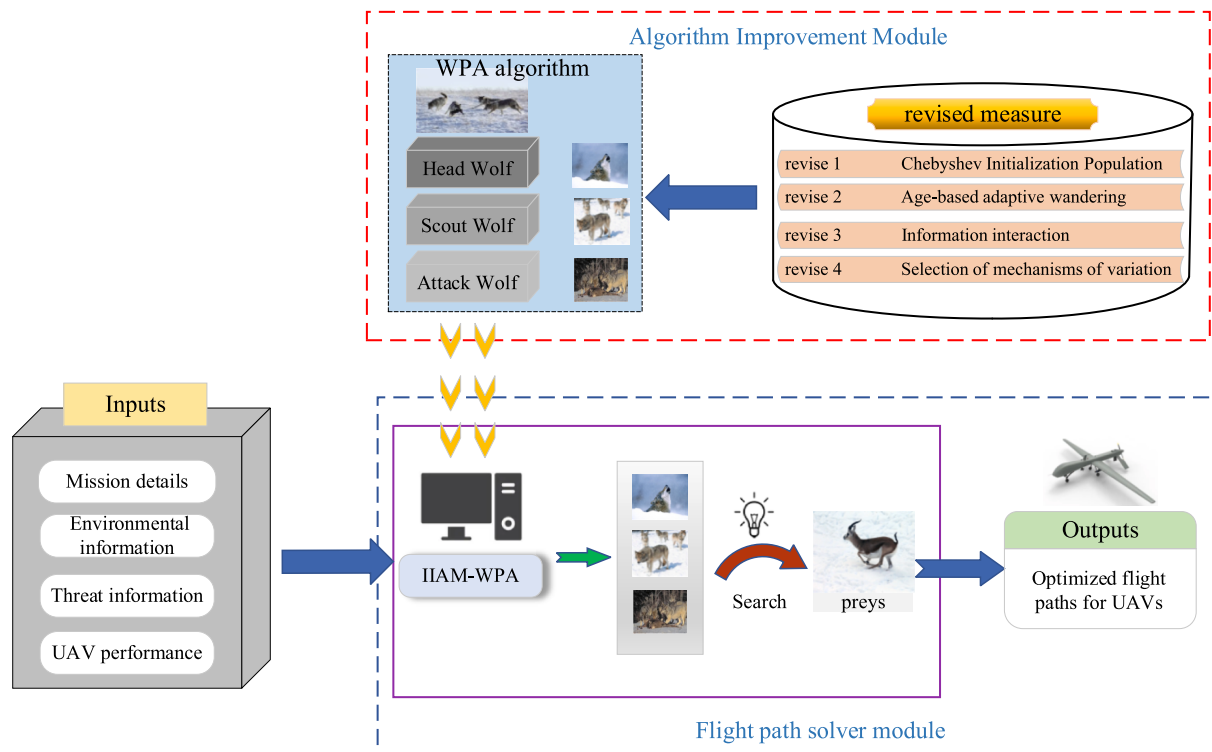


Fig. 5. IIAM-WPA based UAV path planning architecture.

temporal synergy. Spatial synergy refers to maintaining a safe spacing between UAVs during the execution of the mission to prevent collisions. And temporal synergy refers to the need to complete the specified task within the specified time. The synergy constraints can be expressed as follows:

$$\begin{aligned} d_{\min} &\leq d_{ij} \\ t_a &\leq T \end{aligned} \quad (22)$$

Where d_{ij} denotes the distance between UAV i and UAV j ; d_{\min} is the minimum safe distance; t_a is the time for the UAV to complete mission a ; T is the latest time for the mission to be completed.

3. Improved IIAM-WPA trajectory planning

The excellent performance of the WPA has resulted in its rapid development in the field of path planning. However, as task specifications have become increasingly complex, the performance expectations of trajectory planning algorithms have been progressively elevated. The efficacy and precision of the conventional WPA are becoming increasingly challenging (Wang et al., 2020). Accordingly, this paper proposes an enhanced IIAM-WPA algorithm that effectively addresses the shortcomings of traditional WPA, including suboptimal convergence and diminished accuracy.

3.1. Standard wolf pack algorithm

WPA is an optimization algorithm that employs a simulation of the social behavior observed in wolf packs. The wolf pack is divided into three categories of wolves: head wolves, scout wolves and fierce wolves. The hunting process is represented by three distinct behavioral categories, which ensure the survival and development in accordance with the natural selection principle of "survival of the fittest" (Wu & Zhang, 2014). The following is a detailed account of the flow of the wolf pack algorithm. The principle of the wolfpack algorithm is illustrated in Fig. 4, and a detailed description is provided below.

(1) Wolf pack initialization: Positional initialization of artificial wolves in the task space, X_i denotes the i th artificial wolf, X_{\min} and X_{\max} denote the lower and upper bound of the task space.

$$X_i = X_{\min} + rand \times (X_{\max} - X_{\min}), i = 1, 2, \dots, n \quad (23)$$

Where $rand \in (0, 1)$ denotes a random number between 0 and 1.

(2) Head wolf generation: The artificial wolf exhibiting the most effective adaptation is regarded as the head wolf. Head wolf does not engage in predatory behavior until an artificial wolf with superior adaptation supersedes it.

(3) Wandering behavior: The scout wolf will wander in the direction of their prey's strongest scent. This process is repeated until the scout wolf is closer to the prey than the lead wolf, or the maximum number of wanderings is reached. The formula for scout wolf's wandering position is as follows:

$$x_{it}^p = x_{it} + step_a^d \times \sin(2\pi \times p/h) \quad (24)$$

Where x_{it} is the position of the probing wolf in the previous iteration; $step$ is the wandering step size; $h \in [h_{\min}, h_{\max}]$ is an integer; and x_{it}^p is the position of the probing wolf in space after the p th wandering.

(4) Summoning behavior: Following the scout wolf's wander, the head wolf issues call to fierce wolves, prompting a swift response from the latter, and quickly runs to the position of the head wolf. The formula for the running of the fierce wolf is as follows:

$$x_{id}^{k+1} = x_{id}^k + step_b^d \times \frac{g_d^k - x_{id}^k}{|g_d^k - x_{id}^k|} \quad (25)$$

Where x_{id}^k is the spatial position of the fierce wolf in the k th iteration; g_d^k is the spatial position of the head wolf in the k th iteration; and $step_b^d$ is the fierce wolf running step length.

During the fierce wolf run, if it fails to displace head wolf, it will continue to run until the distance between them is less than the

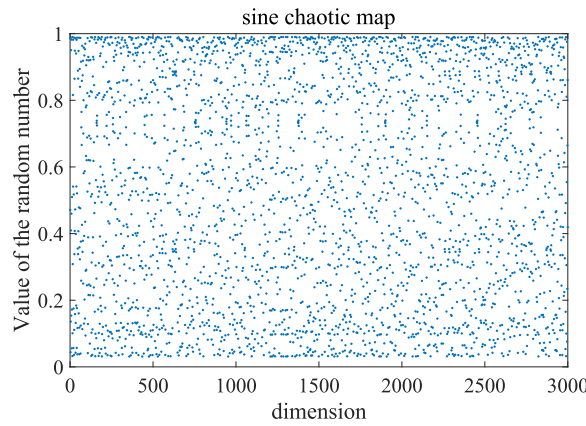


Fig. 6. Sine chaotic mapping image.

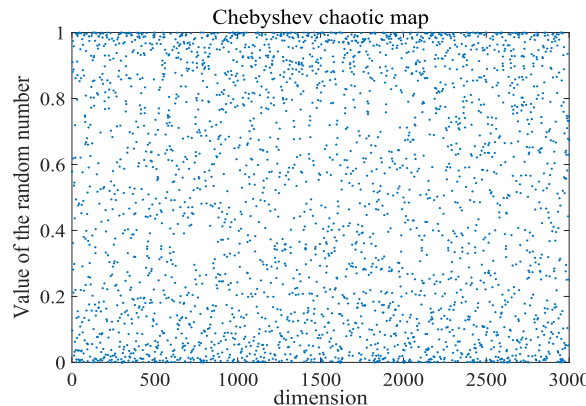
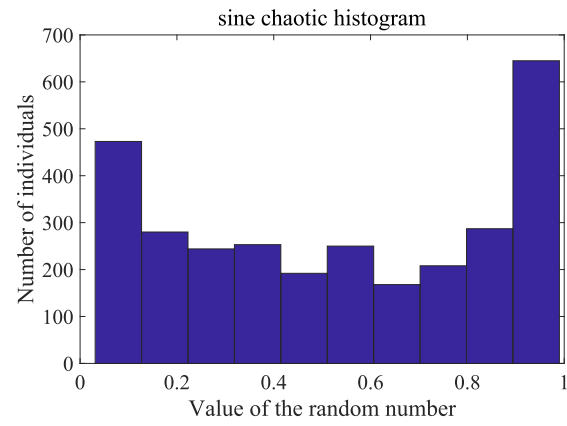


Fig. 7. Chebyshev chaotic mapping image.

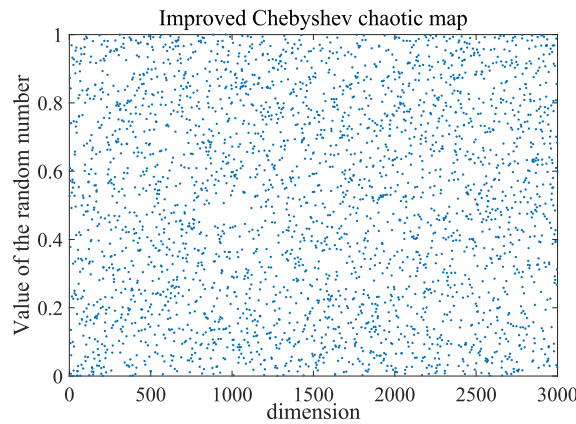
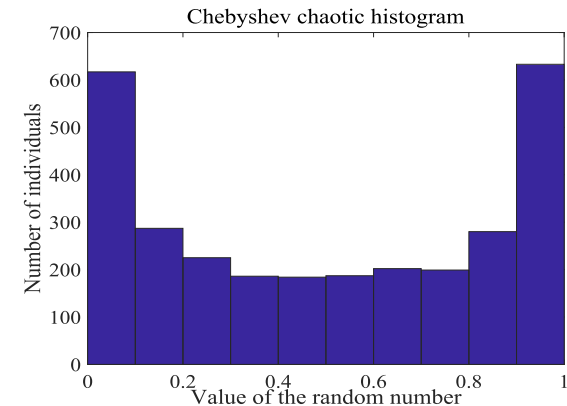
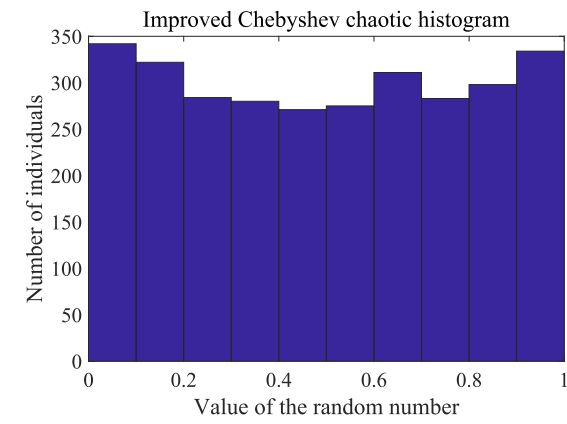


Fig. 8. Improved chebyshev chaotic mapping image.



threshold. The distance between head wolf and fierce wolf as follows:

$$d_{near} = \frac{1}{D \cdot \omega} \sum_{d=1}^D |\max_d - \min_d| \quad (26)$$

Where ω is the distance determination factor; \min_d and \max_d are the upper and lower bounds of the dimensional variables.

(5) Besieging behavior: After a call from head wolf, the head wolf position is regarded as prey, prompting the execution of hunting behavior. The formula for updating position during siege as follows:

$$x_{id}^{k+1} = x_{id}^k + \lambda \cdot step_c^d \times |g_d^k - x_{id}^k| \quad (27)$$

Where $\lambda \in [-1, 1]$, $step_c^d$ is the siege step length of the artificial wolf.

3.2. Information interaction and aging mechanism-based WPA

WPA demonstrates excellent optimization capabilities, rapid convergence, and a certain degree of robustness. However, as the algorithm is applied to increasingly complex optimization problems, certain issues arise:

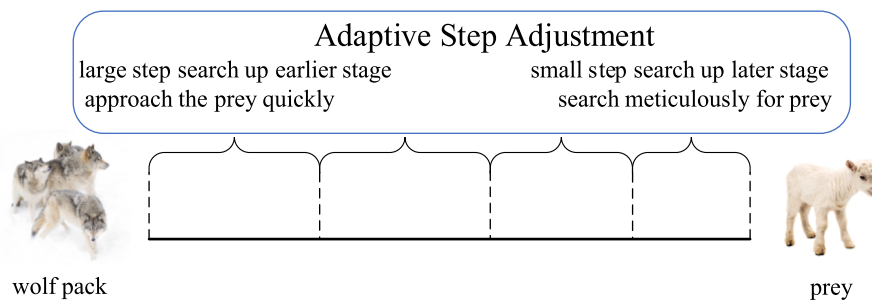


Fig. 9. Adaptive step size adjustment schematic.

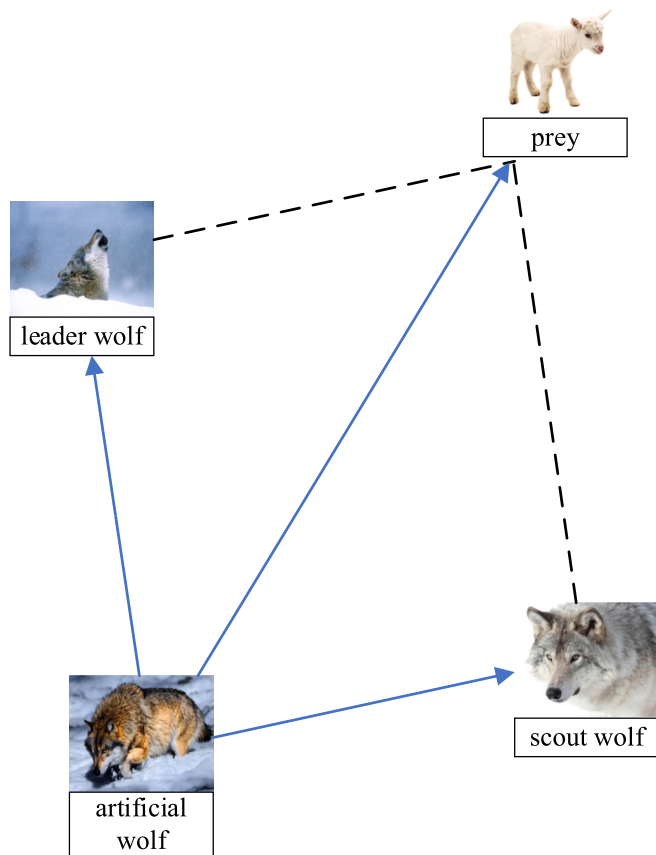


Fig. 10. Information interaction sieve strategy schematic.

- (1) Population aggregation phenomenon: As the algorithmic process continues, the artificial wolves within the population will gradually converge to the head wolf. This results in a reduction of the differences between individuals, which ultimately leads to a stagnation in population evolution;
- (2) Fixed search step: the movement step of each wolf is a fixed value during the predation process, which makes it difficult to ensure the balance of the algorithm between global and local search;
- (3) Lack of information exchange: WPA only searches in the direction of the head wolf during the solving process, and does not interact with excellent individuals in the population. This results in a lack of diversity within the population, which may result in falling into a local optimum trap.

In light of the aforementioned considerations, this chapter proposes an enhanced WPA to address the constrained optimization issue. The proposed algorithmic enhancements are as follows: Firstly, the adoption

of an advanced Chebyshev mapping will serve to augment the dispersion of the population, thereby enhancing the searching capacity; Secondly, the intensification of information exchange between wolves is intended to prevent the loss of valuable data; Lastly, an adaptive wandering strategy and a mutation selection mechanism will be introduced. The schematic of the improved algorithm is shown in Fig. 5.

3.2.1. Improved Chebyshev initialization

The initialisation position of the wolf pack is closely related to the search ability. A good initial distribution will result in a more rapid hunting speed for the wolf pack. However, the conventional WPA employs a random distribution during the initialization phase, which may result in a more concentrated initial position of the wolf pack, thereby impairing the global search ability of the population. Therefore, a suitable initialization method is required to guarantee the quality of the initialised population.

Chaotic mapping is characterised by nonlinearity, randomness and unpredictability. It may be employed as an alternative to pseudo-random number generators for the generation of chaotic sequences (Liu et al., 2021). This paper investigates Chebyshev polynomials and proposes an enhanced Chebyshev chaotic mapping method, which may result in a more dispersed distribution of wolves in the task space. This is represented by the following mathematical formula:

$$\begin{aligned} x(t+1) &= 1 - 2(\cos(2\arccos(x(t))))^2 \\ y(t+1) &= 1 - 2(\cos(2\arccos(y(t))))^2 \\ z(t+1) &= \text{mod}(x(t+1) + y(t+1), 1) \end{aligned} \quad (28)$$

Where $x, y \in [-1, 1]$ and z is the chaos number resulting from the improved Chebyshev mapping.

In order to ascertain the efficacy of the proposed mapping, this section evaluates the proposed mapping method in comparison with the conventional Chebyshev mapping and sine chaotic mapping. The simulation results are illustrated in Fig. 6–8. In the scatter plot, the x-axis represents the scatter dimension, while the y-axis depicts the value taken by the scatter. In the histogram, the x-axis represents the number of scatter points within a given region, while the y-axis depicts the corresponding value of the scatter point.

The simulation results displayed indicate that the enhanced Chebyshev mapping demonstrates a greater propensity for dispersion and a smaller tendency towards clustering when compared to the sinusoidal chaotic mapping and the standard Chebyshev mapping. This observation suggests that its application to the initialization phase of the wolf pack algorithm can enhance the search range of the wolf pack, optimize the local population and accelerate the prey search process.

3.2.2. Adaptive wandering based on age factors

In order to enhance the efficacy of scout wolf wandering and mitigate the potential for local optimality, this section builds upon the traditional wandering methodology and proposes an adaptive wandering strategy that incorporates an age-based factor. The specific measures of improvement as flows:

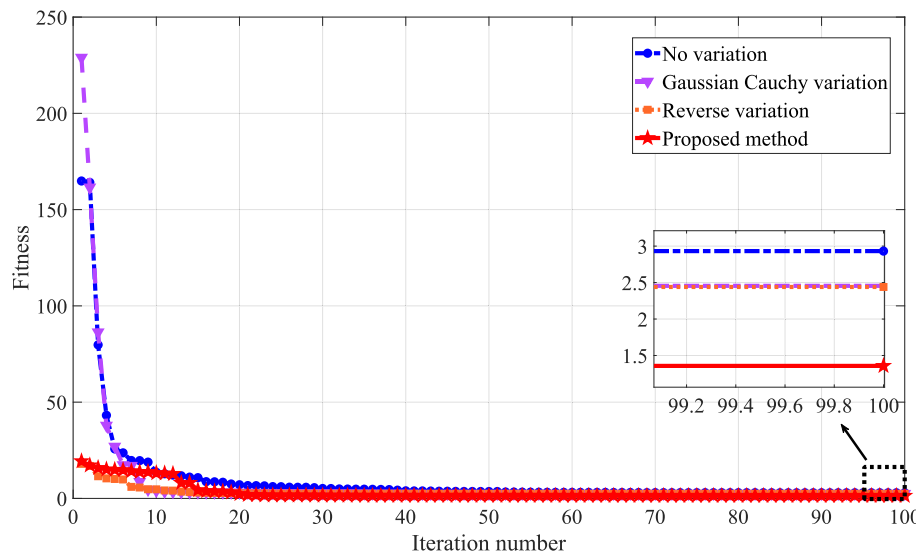


Fig. 11. Comparison of mutation methods.

(1) Adaptive wandering direction adjustment.

In traditional WPA, the search directions of the scout wolf is a fixed value and the search directions are parallel each time. This reduces the exploratory ability of the population, leads to population convergence and loss of variability, and makes it difficult for the algorithm to converge to the global optimum quickly. In order to enhance the efficacy of prey search, this study employs wolf predation in the natural environment as a case study to expand the search radius of the population during the initial stages of wolf predation. This is done with the aim of locating the target trail in a more expeditious manner and determining the principal direction of the search. Furthermore, as the wolf predation process deepens, the location of the prey becomes increasingly clear. This allows the wolf to approach the prey from a single direction, or a few directions, ensuring an efficient hunt. Accordingly, the present study employs an adaptive adjustment of the search direction of the scout wolf, based on the aforementioned mechanism.

$$h = \lfloor (h_{\max} - h_{\min}) * \frac{iter_{now}}{iter_{\max}} + h_{\min} \rfloor \quad (29)$$

Where h is the number of wolf travelling directions; h_{\max} , h_{\min} are the maximum and minimum travelling directions; $iter_{\max}$, $iter_{now}$ represent the maximum and current iteration times, respectively.

(2) Scout wolf deteriorate mechanism.

In the context of a search for a wolf pack, if a scout wolf is unable to approach and capture prey for an extended period, it may be inferred that the individual in question is no longer capable of conducting effective local searches. This phenomenon is reflected in the algorithmic outcome, whereby the optimal position of an individual wolf remains unaltered for an extended period. This indicates that the scout wolf has become disoriented and is persistently deviating from the prey in the incorrect direction. If some scout wolves remain unable to approach the prey after several iterations of the algorithm, it is assumed that there is a possibility of ageing, which increases the risk of local optimality of the population. It is therefore necessary to introduce an age interaction factor to avoid the negative effects of ageing individuals on the population. The ageing individuals will be screened by the age factor, and if the scouting wolf is still unable to escape the local optimum after many optimisations, it will be eliminated along with the artificial wolves that have poor adaptive ability. The objective is to enhance the efficacy of the search process and to guarantee the convergence of the population.

The representation of the scout wolf wandering based on the age interaction factor is as follows:

$$\begin{aligned} x_{it}^p &= x_{it} + step_a^d \times \sin(2\pi \times p/h) + f_a \times rand(0, 1) \times (x_h - x_{it}) \\ f_a &= \frac{F_{it}}{F_h} \end{aligned} \quad (30)$$

Where f_a is the age interaction factor; x_h is the location information of the head wolf in space; F_{it} and F_h are the current fitness values of the scout and head wolf, respectively.

3.2.3. Adaptive adjustment of step length

Traditional WPA has a constant motion step length, which presents a challenge in ensuring the success rate of hunting. In order to enhance the efficacy of wolf predation, the motion step length should be augmented during the preliminary search to expand the search range of the wolf, thereby facilitating the determination of the target location in a more expeditious manner. With the progression of the procedure, the wolves will gradually approach the prey, which may result in the wolves failing to capitalise prey if they do not adapt the motion step length. Accordingly, the motion step length should be adjusted in accordance with the subsequent stages, employing a strategy of progressive refinement. The principle of adaptive adjustment of step length is shown in Fig. 9.

The improved adaptive step is as follows:

$$\begin{aligned} step_a &= \frac{mapRange/S}{1 + 1.5e^{-2.6 * (iter_{\max} - iter_{now}) / iter_{\max}}} \\ step_b &= step_a * 2 \\ step_c &= step_a / 2 \end{aligned} \quad (31)$$

Where $mapRange$ is the range of the task space; S is the wandering step factor; $step_a$ is the adaptive wolf probing wandering step; $iter_{\max}$, $iter_{now}$ are the maximum number of iterations and the current number of iterations, respectively; $step_b$, $step_c$ are the fierce wolf running step and capturing step.

3.2.4. Wolfpack siege based on information interaction

In the context of a siege, the artificial wolf would proceed in a linear fashion towards the head wolf, which could result in a local optimality. In the wild, wolves hunting in packs emit specific calls to convey information to their companions and to facilitate cooperation in the pursuit of prey. In accordance with this biological principle, this section puts forth an information interaction mechanism based on wolf siege,

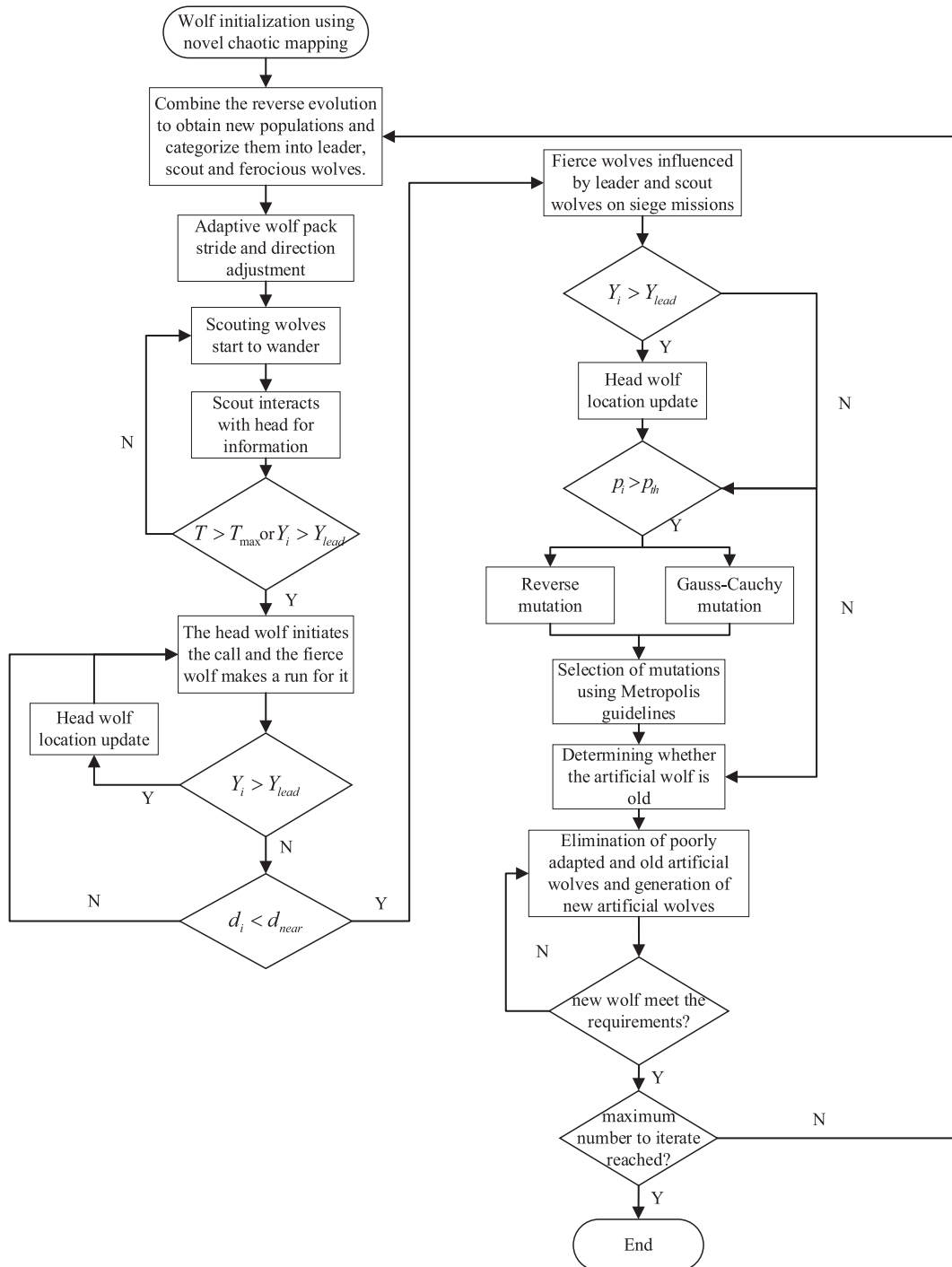


Fig. 12. Flowchart of IIAM-WPA.

Table 1
Algorithm parameterization.

Algorithm type	Main Parameter Setting
WPA	percentage of scout wolves 0.5, step factor 20, number of wandering directions, critical distance, and maximum number of sieges are 10
PSO	Inertia weighted 1.2, social weighted 2, cognitive weighted 2
AFSA	perception range 50, movement maximum step size 3, crowding factor 10
ABC	local optimal decision threshold 5
DE	crossover probability 0.7, mutation probability 0.3

Table 2
UAV and target location information.

UAV departure position	Target position
(20, 10, 0)	(70, 80, 75)
(10, 20, 0)	(85, 95, 60)
(10, 10, 0)	(80, 80, 80)
(15, 30, 0)	(95, 95, 75)

which receives information from other exemplary individuals in the population in addition to the call from the head wolf, and completes the siege of prey with the joint action of both. The following equation rep-

Table 3
Threat barrier parameterization.

Threat type	Threat information
radar detection zone	equipment location R_n (30, 40, 0) maximum vertical measuring distance L_E^n 50
no-fly zone 1	Center (60, 20, 50), radius of action 7
no-fly zone 2	Center (20, 70, 30), radius of action 7
no-fly zone 3	Center (85, 85, 70), radius of action 7
no-fly zone 4	Center (30, 50, 50), radius of action 7
ground no-fly zone 1	ground center position (90, 60) no-fly height 60, radius of action 10

resents the formula for updating the position of the artificial wolf in the siege phase:

$$x_{id}^{k+1} = x_{id}^k + step_c^d \times \left(\lambda \times |g_d^k - x_{id}^k| + (1 - \lambda) \times |x_{jt}^k - x_{id}^k| \right) \quad (32)$$

Where λ is a random number between 0 and 1; $step_c^d$ is the siege step size of the fierce wolf; g_d^k , x_{jt}^k and x_{id}^k are the position information of the head wolf, the scout wolf, and the artificial wolf, respectively.

This method facilitates the preservation and dissemination of valuable information within a population, thereby preventing the loss of effective data and enhancing the diversity of the population, thus avoiding local optimality. A schematic representation of this improvement is provided in Fig. 10.

3.2.5. Reverse Gaussian-Cauchy variation

WPA exhibits a positive feedback effect in the later stages of the search. The lead wolf acts as a guiding force for the entire pack, causing the artificial wolves to gradually converge toward it. This convergence reduces individual differences, ultimately leading to evolutionary stagnation.

To address this issue, this section proposes a reverse Gaussian-Cauchy mutation method. This approach enhances population diversity and prevents premature convergence by introducing perturbations to generate new offspring in the later stages of the algorithm. After the artificial wolf completes the hunting behaviour, it will determine

whether to perform mutation operation based on a dynamically changing mutation probability and will select the appropriate mutation method according to the Metropolis criterion.

Among the available variation strategies, Gaussian and Cauchy variations are two commonly employed approaches that introduce perturbations to help individuals escape from local optima and enhance the algorithm's search capability (Ou et al., 2022; Wang et al., 2022c). To improve population diversity and the algorithm's search ability, this section combines Gaussian variation with Cauchy variation. The mathematical expression for the Gauss-Cauchy variation is as follows:

$$x_{im} = x_i \cdot (1 + \eta_1 \text{Gauss}(0, \sigma^2) + \eta_2 \text{Cauchy}(0, \sigma^2))$$

$$\sigma = \begin{cases} 1, & f(x_{best}) < f(x_i) \\ \exp\left(\frac{f(x_{best}) - f(x_i)}{|f(x_{best})|}\right), & \text{otherwise} \end{cases} \quad (33)$$

Where x_i and x_{im} represent the current position and the position after mutation, respectively; σ^2 denotes the standard deviation of the Gauss-Cauchy mutation strategy; η_1 and η_2 are the dynamic parameters of adaptive mutation, respectively.

To increase population diversity, a reverse evolution mechanism is added to the above variants. This is achieved by mapping the current solution to the reverse space, which facilitates convergence and mitigates the risk of local optimization.

The methodology of the reverse Gaussian-Cauchy mutation is as follows: an adaptive mutation jump rate is initially established. If a randomly generated number is less than this rate, the mutation operation is not performed. Conversely, if the random number exceeds the specified mutation rate, the mutation operation is applied to the wolves, and the resulting fitness value is subsequently calculated. Subsequently, the Metropolis criterion is employed to ascertain whether the Gaussian-Cauchy mutation should be accepted. In accordance with the Metropolis criterion, the acceptance probability is as follows:

$$p = \begin{cases} 1, & F(n+1) < F(n) \\ \exp\left(-\frac{F(n+1) - F(n)}{T}\right), & F(n+1) \geq F(n) \end{cases} \quad (34)$$

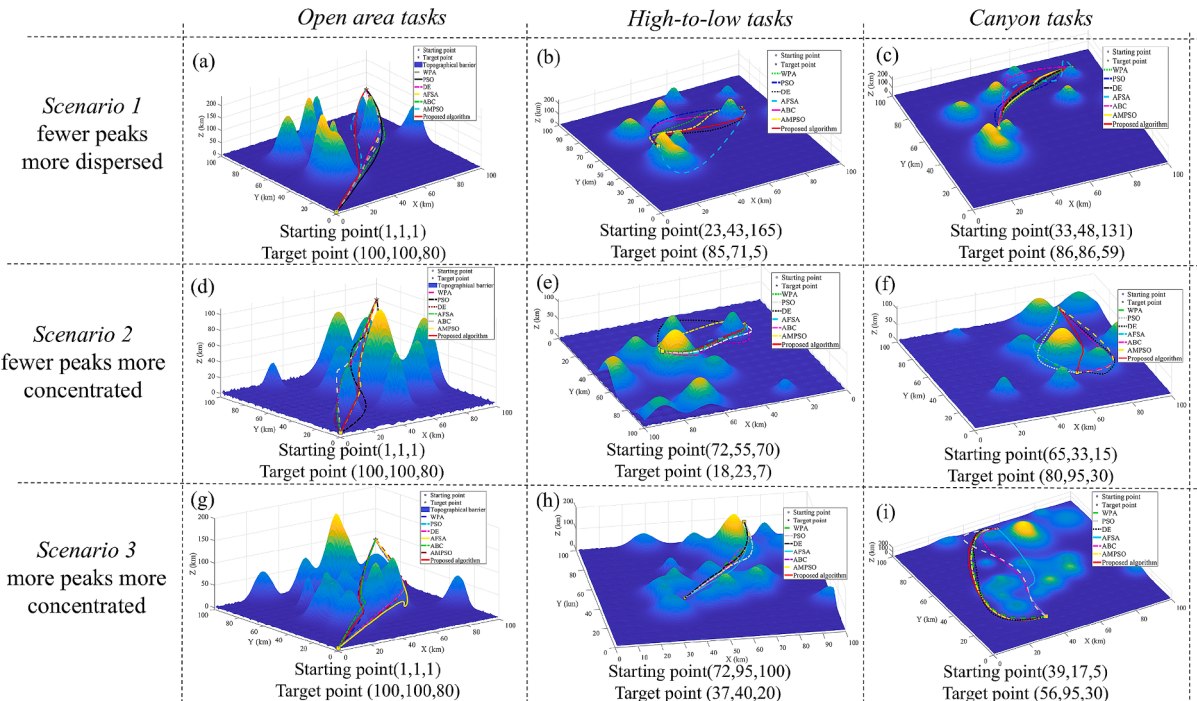


Fig. 13. Task scenario simulation.

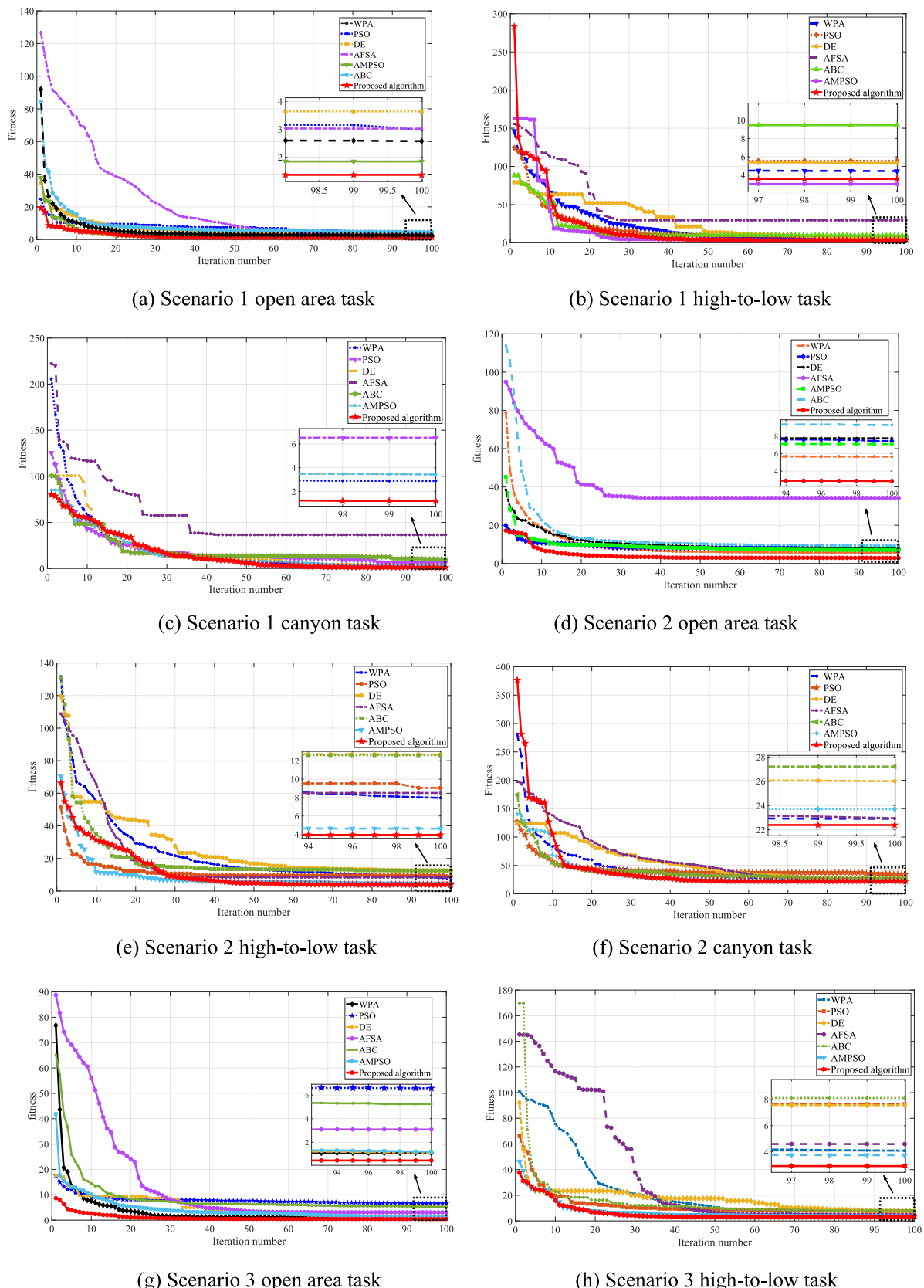
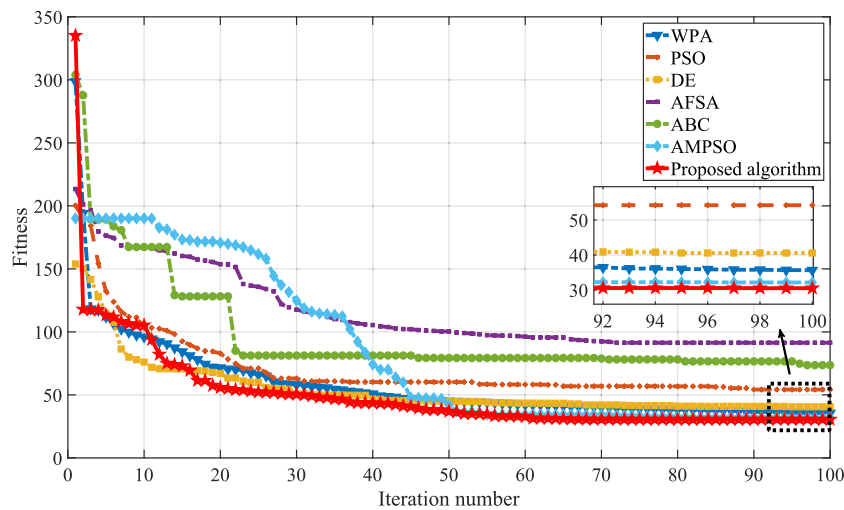


Fig. 14. Comparison of simulation adaptation.



(i) Scenario 3 canyon task

Fig. 14. (continued).

Where $F(n+1)$ and $F(n)$ are the fitness after Gaussian Cauchy variation and reverse variation, respectively; T is the temperature, which is used to control the selection probability, and an exponential descent strategy is used in this paper.

In order to ascertain the efficacy of the proposed methodology, this paper employs multiple mutation methods for comparative simulation under identical parameters. The simulation results are shown in Fig. 11.

As demonstrated in Fig. 11, Gaussian Cauchy mutation can address the local optimal problem to a certain extent. Nevertheless, the method employing this mutation strategy demonstrates suboptimal adaptation in the initial stage, with the wolf packs requiring greater energy expenditure to approach the prey. Conversely, the reverse mutation strategy demonstrates superior performance in the initial stage but exhibits diminished search ability in subsequent iterations of the update. Accordingly, this paper integrates the aforementioned two variation techniques with the objective of enhancing the algorithm's search capacity. As evidenced by the simulation outcomes, the proposed methodology exhibits superior planning outcomes and effectively precludes premature convergence of the populations.

Combining the above improvements, the IIAM-WPA flowchart is shown in Fig. 12.

4. Algorithm simulation analysis

In this chapter, we employ the proposed method for simulating UAV trajectory planning in mountainous environments. We then proceed to verify the effectiveness of the proposed method by comparing the results with a range of established trajectory planning algorithms. The process is outlined below: (1) Initially, the threat information, including the mission environment, no-fly zone, radar detection area, and other pertinent details, is obtained based on space-based detection data. Subsequently, this information is employed in the construction of a three-dimensional mission space environment model; (2) A trajectory planning methodology is employed to undertake global trajectory planning within the task space and to supplement the task space based on the acquired information; (3) Subsequently, the secure and viable route is determined.

4.1. Parameter configuration

The computer configuration used for the simulation test in this paper

is Intel Core i5 processor (2.10 GHz), 16 GB RAM and Windows 11 (64-bit) operating system, and the simulation test of UAV trajectory planning is carried out using WPA, PSO, AFSA, ABC, DE, and the method proposed in this paper under the device, and the specific parameters of the simulation are as follows.

In order to ensure the comparability of the planning results, this paper will be simulated under the premise of the same task environment, population size, and number of iterations, with the same parameter settings: The population size is all 50 in all cases, the number of iterations is 100 in all cases, and the specific parameter settings for each algorithm are listed in the Table 1.

Table 2 provides a summary of the pertinent information regarding enemy and friendly positions in relation to the multi-UAV mission.

Table 3 presents the threat barrier information for the collaborative task scenarios.

4.2. Simulation results and analysis

UAV is employed in the performance of complex missions due to its favourable characteristics in terms of manoeuvrability and safety. Meanwhile the complexity of mountainous environments presents significant difficulties and challenges in multi-UAV target tracking. The aim of this study is to address the issue of autonomous tracking trajectory planning for UAVs in mountainous environments. Additionally, the effectiveness of IIAM-WPA in UAV path planning is to be verified.

The mission space is defined as $100 \text{ km} \times 100 \text{ km} \times 250 \text{ km}$, and the detailed environmental and mission information are presented in Tables 2–3. The performance of PSO, WPA, ABC, AFSA, DE, and the proposed method is evaluated in diverse mission environments, with the parameter settings of the algorithms presented in Table 1. In addition, the following assumptions are made for the experiments in each scenario: 1) it is assumed that the global environmental information of the UAV is known during flight; 2) it is assumed that the performance limitations of the UAV in each simulated scenario are the same.

In order to verify the effectiveness of the proposed method in different complex mission environments, three different mission terrains have been randomly generated in this chapter. The characteristics of these terrains are as follows: the first mission scenario has a smaller number of peaks, and the distribution of the peaks is more dispersed, which makes it easier for the UAV to complete. The second mission scenario has a smaller number of peaks but a more centralised distribution, which will present a greater challenge for the UAV to complete

Table 4
Task simulation result parameters.

Task scenario	Algorithm	Optimal value	Worst value	Average value	Variance value
Scenario 1 open area task	WPA	1.7592	2.9316	2.5697	0.4694
	PSO	2.4928	3.1622	2.9789	0.2578
	DE	1.6526	7.3315	3.6383	1.9558
	AFSA	1.5768	7.4093	3.0197	1.7040
	ABC	3.2789	8.3004	4.6223	2.1537
	AMPSO	1.6642	3.2566	1.8412	0.4777
	Proposed method	1.3574	1.4195	1.3687	0.0196
Scenario 1 high-to-low task	WPA	3.6098	5.7402	4.4409	0.7291
	PSO	4.7857	6.1536	5.5648	0.3097
	DE	4.1995	9.9253	5.3447	6.5569
	AFSA	23.2249	35.5233	29.6362	19.8989
	ABC	5.9366	10.8520	9.4501	4.0579
	AMPSO	2.9901	3.0908	3.0304	0.0030
	Proposed method	3.5138	3.6844	3.5769	0.0076
Scenario 1 canyon task	WPA	1.5311	3.5143	2.8836	0.5570
	PSO	4.2982	9.6569	6.5298	3.0647
	DE	2.2062	3.8466	3.4378	0.5046
	AFSA	35.0814	40.1500	36.5777	5.0797
	ABC	7.7747	13.9771	10.2865	11.3525
	AMPSO	2.7712	4.6750	3.4235	0.5353
	Proposed method	0.9524	1.5621	1.1963	0.1115
Scenario 2 open area task	WPA	2.8531	8.1004	5.6487	1.8417
	PSO	6.4064	15.8493	7.434	2.8110
	DE	6.4353	9.4767	7.2232	0.7725
	AFSA	17.8505	62.1293	34.2664	14.4730
	ABC	7.2018	15.1156	9.2696	2.2670
	AMPSO	5.2987	7.2884	7.0656	0.5933
	Proposed method	2.8634	2.8760	2.8646	0.0038
Scenario 2 high-to-low task	WPA	6.7674	9.1959	7.9687	1.4752
	PSO	7.0958	10.1477	9.0507	1.7472
	DE	11.9256	13.1786	12.6774	0.4711
	AFSA	6.8869	11.0471	8.5001	2.9494
	ABC	10.7850	14.2376	12.6037	3.5575
	AMPSO	4.2215	4.7515	4.6204	0.0527
	Proposed method	3.8295	4.0333	3.9302	0.0089
Scenario 2 canyon task	WPA	22.5020	24.1643	22.9037	0.5017
	PSO	32.7059	36.0185	34.7608	1.7893
	DE	24.2256	31.4992	26.0085	9.4772
	AFSA	21.3447	27.8038	22.9518	7.4469
	ABC	23.7208	30.9400	27.2285	8.1807
	AMPSO	23.3493	25.1030	23.7000	0.6151
	Proposed method	22.2877	22.4368	22.3882	0.0048
Scenario 3 open area task	WPA	0.6251	2.8531	1.0978	0.8781
	PSO	1.8017	8.9628	6.5749	1.9303
	DE	0.9654	1.1463	1.1282	0.0543
	AFSA	0.4159	23.7354	3.0849	6.9216
	ABC	2.6516	9.9879	5.2390	2.1409
	AMPSO	0.5991	1.5981	1.2073	0.3473
	Proposed method	0.3949	0.6366	0.4584	0.0977
Scenario 3 high-to-low task	WPA	3.1660	6.3516	4.0882	1.7636
	PSO	5.7972	11.2541	7.6576	4.7374
	DE	5.8953	10.0706	7.5654	5.2299
	AFSA	2.9706	10.8426	4.5882	12.2252
	ABC	3.8135	11.5914	8.1235	8.4924
	AMPSO	3.5652	4.1559	3.7399	0.0591
	Proposed method	2.8554	2.9451	2.9022	0.0012
Scenario 3 canyon task	WPA	34.2355	37.1159	35.6419	1.0404
	PSO	49.8905	58.1640	54.2218	14.4224
	DE	36.1285	46.1406	40.5674	21.8565
	AFSA	83.6314	94.6554	91.3894	19.1776
	ABC	69.9109	80.8564	73.6209	22.8441
	AMPSO	31.1726	36.0019	32.1384	4.6644
	Proposed method	30.4992	30.5665	30.5262	0.0014

the mission; the third mission scenario has a larger number of peaks and a more centralised distribution, which will also present a greater challenge for the UAV to complete the mission. In order to demonstrate the efficacy of the proposed method in performing different tasks, seven different methods are adopted to perform the open scene task, the high-to-low task, and the canyon task in the above three mission terrains. The scenes are methodically categorised according to the terrain and task types. These classifications function as the horizontal and vertical axes of the images, thus facilitating analysis. The combination of these scenes enables the acquisition of simulation results, illustrating the response scenarios depicted in Fig. 13.

As demonstrated in the results of Fig. 13, seven planning methods are employed in this section to simulate UAV flight trajectories under nine different mission scenarios. The simulation results demonstrate the efficacy of the proposed method in determining UAV flight trajectories quickly and efficiently under a variety of mission scenarios, including both challenging and straightforward ones. In order to provide further illustration of the effectiveness of the proposed method, the simulation results for each scenario are analysed and compared according to the terrain and the type of mission, as demonstrated in Fig. 14 and Table 4.

From the task planning results shown in Fig. 14 and Table 4, it can be seen that the proposed method is not always the best-performing method in the initial stage, but that the proposed method does have a good local optimisation ability, being capable of finding the better path in subsequent stages of evolution. It is noteworthy that the proposed method consistently yields optimal planning outcomes across all eight scenarios. In addition, in the canyon task of Task Scenario 1, the proposed method obtained a path adaptation of 1.1963, while the AFSA method obtained an adaptation of 36.5777, achieving a highest fitness improvement of about 96.73 % in this scenario, thus demonstrating the effectiveness of the proposed method. Moreover, the proposed method demonstrated reduced variance in multiple simulation experiments when compared to alternative algorithms, thereby validating its reliability.

The preceding simulations substantiate the efficacy of the proposed method. In order to further illustrate the advantages of the proposed method in multi-UAV missions, the following simulations have been performed, the results of which are presented hereafter.

Fig. 15–17 illustrate the planning paths obtained using the AMPSO algorithm, the standard WPA, and the proposed improved algorithm under complex threat conditions. It can be observed that all three methods are capable of generating a safe flight path for multiple UAVs. Nevertheless, the planning path obtained by the AMPSO method exhibits a considerable turning angle and a high number of turns, which will result in a significant energy expenditure by the UAV and simultaneously necessitates the UAV's maneuverability; The planning path obtained by the standard WPA has a reduced number of turns, yet some of these turns are superfluous. To illustrate, a non-essential turn occurs during the approach to the target point in planning path 4. Furthermore, the proposed algorithm requires the least number of resources, as demonstrated by the Fig. 17, which illustrates that its planned paths are aligned with the edges of the obstacles and maintain a safe distance from them, thereby reducing energy consumption. Furthermore, the number of turns is reduced, as is their magnitude. In order to present the planning results of the three methods in a more intuitive manner, this paper compares the lengths of the flight paths obtained from the planning of the three methods. The total flight distances depicted in Figs. 15–17 are 519.628 km, 518.931 km, and 499.284 km, respectively. In the simulation scenario previously referenced, the ideal shortest path, defined as the straight-line distance, is 488.387 km. The deviation of the planning results of the aforementioned three methods from the optimal result is 6.4 %, 6.2 % and 2.2 %, respectively. It is evident that the proposed method exhibits a greater propensity to approximate the ideal flight trajectory in the context of multi-UAV planning, which further corroborates the effectiveness and advantages of the proposed method in multi-UAV planning. However, the course of the study also revealed

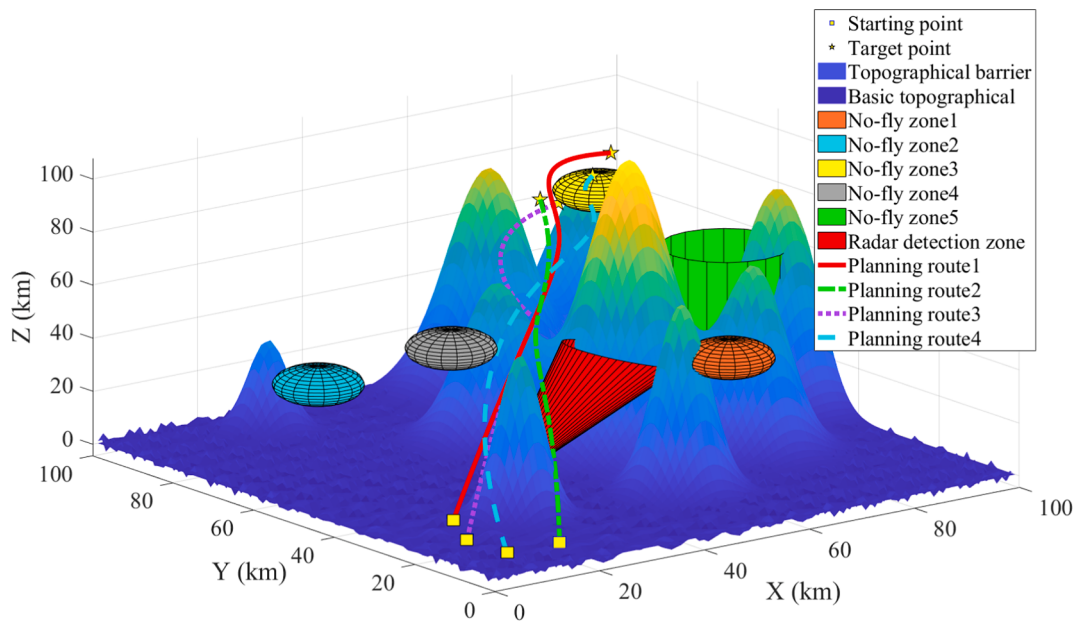


Fig. 15. AMPSO planning results.

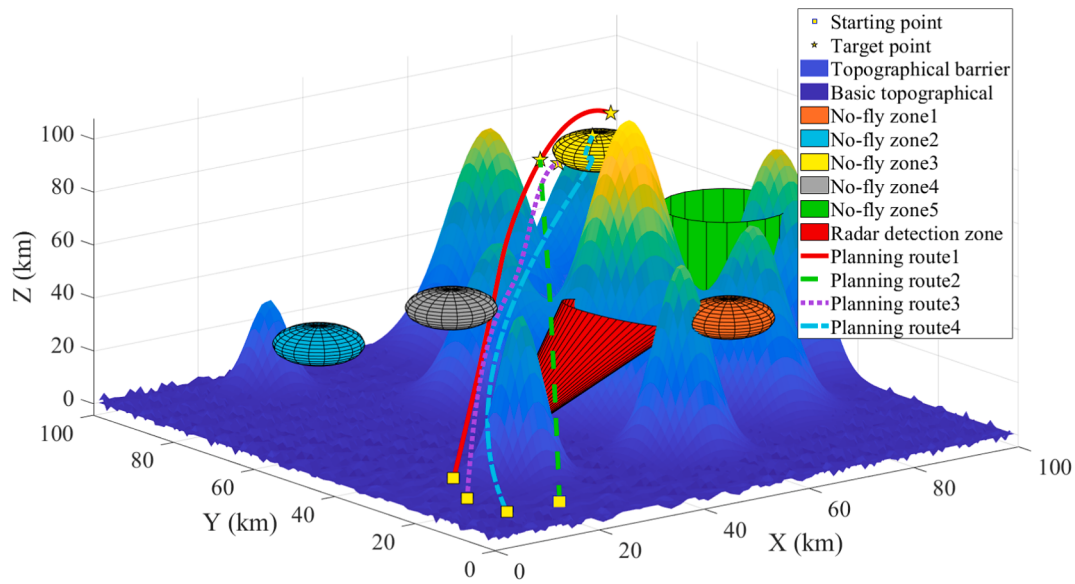


Fig. 16. WPA planning results.

certain shortcomings and limitations of the current study, which are summarised as follows:

Firstly, the information regarding the mission environment is known, i.e. the primary focus of this paper is multi-UAV global path planning, which has certain limitations in terms of addressing dynamic emergent problems. It is difficult to ensure the efficiency of planning when solving highly dynamic mission problems. Additionally, the present method will also be affected by the results of initialization, and a poorer initial quality will affect the efficiency of planning. In subsequent research, the focus will be on the UAV cluster flight task under a high dynamic task posture, enabling the UAV to modify its flight trajectory quickly to ensure flight safety. Simultaneously, efforts will be made to further mitigate the impact of initialization on the optimization seeking ability, enhancing the stability of the planning method.

Secondly, the research in this paper principally focuses on the UAV planning level, i.e. to ensure the feasibility of the UAV planning

trajectory according to the dynamics constraints during the planning process, and to provide the reference trajectory for the subsequent real flight. However, in real flight missions, in order to ensure the normal flight of UAVs, it is also necessary to consider the configuration of UAV formations under different mission situations. At the same time, in order to ensure the safety of UAV flight, it is necessary to track and control the reference trajectory and to obtain the control parameters required by the UAV at each moment. The subsequent research will focus on the UAV formation configuration and control problems.

The simulation of UAV trajectory planning in the aforementioned multiple scenarios demonstrates that the proposed algorithm enhances the planning outcomes and stability, in both single UAV and multi-UAV coordinated trajectory planning. This evidence substantiates the efficacy of the proposed method in addressing the multi-UAV trajectory planning problem.

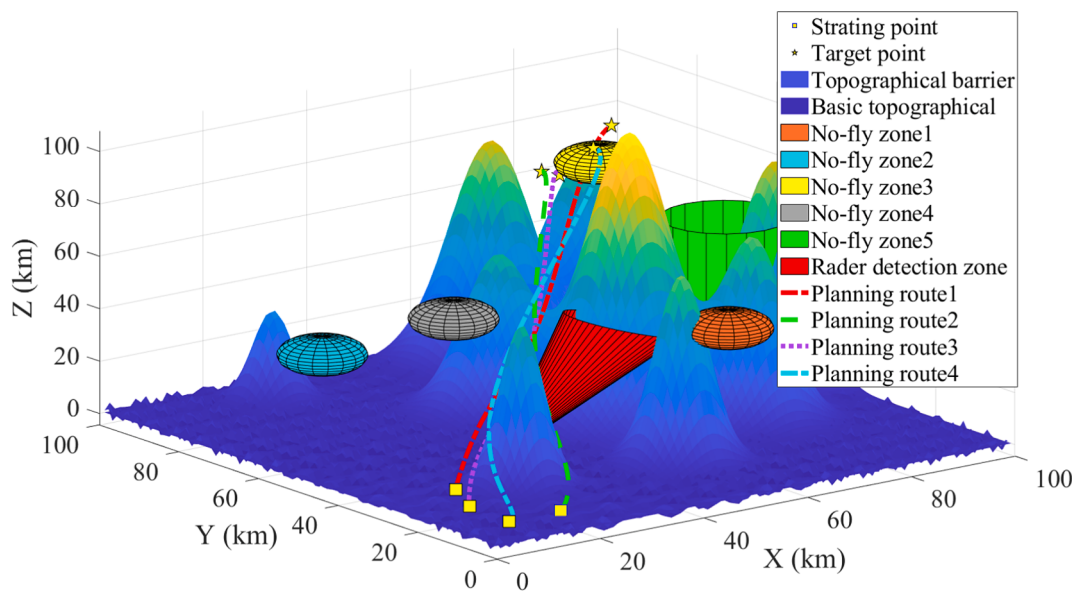


Fig. 17. IIAM-WPA planning results.

5. Conclusion

To address the issues of inadequate planning, imprecise trajectory planning, and inefficiency, this paper proposes an aging wolf pack algorithm based on information interaction and successfully applies it to multi-UAV trajectory planning. This marks the first research effort to use the WPA in conjunction with an aging mechanism to solve constrained optimization problems. Given the numerous potential threats that may arise during real-world missions, this paper presents a method for transforming UAV global trajectory planning into a multi-constraint optimization problem.

The IIAM-WPA utilizes an enhanced Chebyshev mapping during the initialization phase to optimize the dispersion of the initialized wolf pack positions and accelerate the algorithm's convergence. Additionally, an adaptive wolf wandering method based on the age factor is proposed. This method employs a “coarse to fine” wandering strategy and adaptively adjusts the number of wandering directions to balance the relationship between global and local searches. Concurrently, the age factor is introduced to enhance the aging wolves and augment the diversity of the population. During the wolf siege process, the interaction of information with the most exemplary individuals of the population is intensified, while mutation perturbation is employed to assist the population in evading the local optimal trap. To assess the efficacy of the proposed methodology, this study conducts ten independent simulation experiments for each of the methods across multiple distinct mission scenarios. The results demonstrate that the proposed trajectory planning algorithm can successfully identify a flyable path. Moreover, a comparative analysis with WPA, PSO, DE, AFSA, ABC and other optimisation algorithms is conducted. In the single UAV task, the proposed method achieves the highest improvement of 96.73 % compared to other methods, and in the multi-UAV planning task, the proposed method achieves 4.2 % and 4 % improvement compared to AMPSO and WPA, respectively. This verifies the validity of the proposed algorithm in terms of UAV trajectory planning and its advantages.

CRediT authorship contribution statement

Jinyu Zhang: Conceptualization, Methodology, Software, Visualization, Writing – original draft. **Xin Ning:** Conceptualization, Resources. **Shichao Ma:** Supervision, Methodology, Writing – review & editing. **Rugang Tang:** Conceptualization, Writing – review & editing.

Declaration of competing interest

The authors declare that they have no known competing financial interests or personal relationships that could have appeared to influence the work reported in this paper.

Acknowledgements

This project was sponsored by Youth Science Foundation of the National Natural Science Foundation of China (No. 12402038) and the Xi'an Key Laboratory of Aircraft Optical Imaging and Measurement Technology (No. 2023-001). The authors are very grateful to the reviewers for their valuable comments and suggestions.

Data availability

Data will be made available on request.

References

- Cabreira, T. M., Brisolara, L. B., & Paulo, R. F. (2019). Survey on coverage path planning with unmanned aerial vehicles. *Drones*, 3(1), 4. <https://doi.org/10.3390/drones3010004>
- Campo, L. V., Ledezma, A., & Corrales, J. C. (2020). Optimization of coverage mission for lightweight unmanned aerial vehicles applied in crop data acquisition. *Expert Systems With Applications*, 149, Article 113227. <https://doi.org/10.1016/j.eswa.2020.113227>
- Chen, L., Shan, Y. X., Tian, W., Li, B. J., & Cao, D. P. (2018). A fast and efficient double-tree RRT*-like sampling-based planner applying on mobile robotic systems. *IEEE-ASME Transactions on Mechatronics*, 23(6), 2568–2578. <https://doi.org/10.1109/TMECH.2018.2821767>
- Chen, X. Q., Li, Z. B., Yang, Y. S., Qi, L., & Ke, R. M. (2021). High-resolution vehicle trajectory extraction and denoising from aerial videos. *IEEE Transactions on Intelligent Transportation Systems*, 22(5), 3190–3202. <https://doi.org/10.1109/TITS.2020.3003782>
- Fu, J. F., Núñez, A., & De Schutter, B. (2022). Real-time UAV routing strategy for monitoring and inspection for postdisaster restoration of distribution networks. *IEEE Transactions on Industrial Informatics*, 18(4), 2582–2592. <https://doi.org/10.1109/TII.2021.3098506>
- Fuertes, D., Del-Blanco, C. R., Jaureguizar, F., Navarro, J. J., & García, N. (2023). Solving routing problems for multiple cooperative Unmanned Aerial Vehicles using Transformer networks. *Engineering Applications of Artificial Intelligence*, 122, Article 106085. <https://doi.org/10.1016/j.engappai.2023.106085>
- Ha, I. K. (2024). Improved A-star search algorithm for probabilistic air pollution detection using UAVs. *Sensors*, 24(4), 1141. <https://doi.org/10.3390/s24041141>
- Jeong, I. B., Lee, S. J., & Kim, J. H. (2019). Quick-RRT*: Triangular inequality-based implementation of RRT* with improved initial solution and convergence rate. *Expert Systems with Applications*, 123, 82–90. <https://doi.org/10.1016/j.eswa.2019.01.032>

- Kang, M. L., Chen, Q. H., Fan, Z. M., Yu, C., Wang, Y. X., & Yu, X. J. (2024). A RRT based path planning scheme for multi-DOF robots in unstructured environments. *Computers and Electronics in Agriculture*, 218, Article 108707. <https://doi.org/10.1016/j.compag.2024.108707>
- Krishnan, S., Boroujerdian, B., Fu, W., Faust, A., & Reddi, V. J. (2021). Air Learning: A deep reinforcement learning gym for autonomous aerial robot visual navigation. *Machine Learning*, 110(9), 2501–2540. <https://doi.org/10.1007/s10994-021-06006-6>
- Kyriakakis, N. A., Marinaki, M., Matsatsinis, N., & Marinakis, Y. (2022). A cumulative unmanned aerial vehicle routing problem approach for humanitarian coverage path planning. *European Journal of Operational Research*, 300(3), 992–1004. <https://doi.org/10.1016/j.ejor.2021.09.008>
- Lee, D. H., & Ahn, J. (2024). Multi-start team orienteering problem for UAS mission re-planning with data-efficient deep reinforcement learning. *Applied Intelligence*, 54(6), 4467–4489. <https://doi.org/10.1007/s10489-024-05367-4>
- Li, B., Gan, Z. G., Chen, D. Q., & Aleksandrovich, D. S. (2020). UAV maneuvering target tracking in uncertain environments based on deep reinforcement learning and meta-learning. *Remote Sensing*, 12(22), 3789. <https://doi.org/10.3390/rs12223789>
- Li, Y. Y., Guan, Q. F., Gu, J. F., Jiang, X. T., & Li, Y. (2024). A hierarchical deep reinforcement learning method for solving urban route planning problems under large-scale customers and real-time traffic conditions. *International Journal of Geographical Information Science*, 2024, 1–24. <https://doi.org/10.1080/13658816.2024.2413394>
- Lin, Y. S., Hue, G., Wang, L., Li, Q. S., & Zhu, J. W. (2024). A multi-AGV routing planning method based on deep reinforcement learning and recurrent neural network. *IEEE-CAA Journal of Automatica Sinica*, 11(7), 1720–1722. <https://doi.org/10.1109/JAS.2023.123300>
- Liu, B., Ni, W., Liu, R. P., Guo, Y. J., & Zhu, H. B. (2023). Optimal routing of unmanned aerial vehicle for joint goods delivery and in-situ sensing. *IEEE Transactions on Intelligent Transportation Systems*, 24(3), 3594–3599. <https://doi.org/10.1109/TITS.2022.3225269>
- Liu, C. Y., Xie, S. B., Sui, X., Huang, Y., Ma, X. Q., Guo, N., & Yang, F. (2023). PRM-D* method for mobile robot path planning. *Sensors*, 23(7), 3512. <https://doi.org/10.3390/s23073512>
- Liu, G. Y., Shu, C., Liang, Z. W., Peng, B. H., & Cheng, L. F. (2021). A modified sparrow search algorithm with application in 3d route planning for UAV. *Sensors*, 21(4), 1224. <https://doi.org/10.3390/s21041224>
- Ning, Z. L., Hu, H., Wang, X. J., Guo, L., Guo, S., Wang, G. Y., & Gao, X. B. (2024). Mobile edge computing and machine learning in the internet of unmanned aerial vehicles: A survey. *ACM Computing Surveys*, 56(1), 13. <https://doi.org/10.1145/3604933>
- Ou, X. F., Wu, M., Pu, Y. Y., Tu, B., Zhang, G. Y., & Xu, Z. (2022). Cuckoo search algorithm with fuzzy logic and Gauss-Cauchy for minimizing localization error of WSN. *Applied Soft Computing*, 125, Article 109211. <https://doi.org/10.1016/j.asoc.2022.109211>
- Peng, Q., Wu, H. S., Li, N., & Wang, F. (2024). A Dynamic Task Allocation Method for Unmanned Aerial Vehicle Swarm Based on Wolf Pack Labor Division Model. *IEEE Transactions on Emerging Topics in Computational Intelligence*, 8(6), 4075–4089. <https://doi.org/10.1109/TETCI.2024.3386614>
- Rouillon, S., Desaulniers, G., & Soumis, F. (2006). An extended branch-and-bound method for locomotive assignment. *Transportation Research Part B-Methodological*, 40(5), 404–423. <https://doi.org/10.1016/j.trb.2005.05.005>
- Shao, S. Y., Wang, L. W., Yan, X. H., & Wu, Q. X. (2023). Trajectory planning and prescribed performance tracking control based on fractional-order observers for unmanned helicopters with unmeasurable states. *Aerospace Science and Technology*, 139, Article 108360. <https://doi.org/10.1016/j.ast.2023.108360>
- She, A. Q., Wang, L. J., Peng, Y. L., & Li, J. H. (2023). Structural reliability analysis based on improved wolf pack algorithm AK-SS. *Structures*, 57, Article 105289. <https://doi.org/10.1016/j.istruc.2023.105289>
- Song, Q. S., Yu, L. Y., Li, S. B., Hanajima, N., Zhang, X. X., & Pu, R. Q. (2023). Energy Dispatching Based on an Improved PSO-ACO Algorithm. *International Journal of Intelligent Systems*, 2023, Article 3160184. <https://doi.org/10.1155/2023/3160184>
- Wan, P. F., Wang, S. K., Xu, G. Y., Long, Y. Y., & Hu, R. Q. (2024). Hybrid Heuristic-Based Multi-UAV Route Planning for Time-Dependent Data Collection. *IEEE Internet of Things Journal*, 11(13), 24134–24147. <https://doi.org/10.1109/JIOT.2024.3390732>
- Wang, D. X., Ban, X. J., Ji, L. H., Guan, X. Y., Liu, K., & Qian, X. (2020). An Adaptive Shrinking Grid Search Chaotic Wolf Optimization Algorithm Using Standard Deviation Updating Amount. *Computational Intelligence and Neuroscience*, 2020, Article 7986982. <https://doi.org/10.1155/2020/7986982>
- Wang, J. Y., Li, Y. H., Li, R. X., Chen, H., & Chu, K. J. (2022). Trajectory planning for UAV navigation in dynamic environments with matrix alignment Dijkstra. *Soft Computing*, 26(22), 12599–12610. <https://doi.org/10.1007/s00500-022-07224-3>
- Wang, M. H., & Ma, Y. J. (2023). A differential evolution algorithm based on accompanying population and piecewise evolution strategy. *Applied Soft Computing*, 143, Article 110390. <https://doi.org/10.1016/j.asoc.2023.110390>
- Wang, W., Wang, L., Wu, J. F., Tao, X. P., & Wu, H. J. (2022). Oracle-Guided Deep Reinforcement Learning for Large-Scale Multi-UAVs Flocking and Navigation. *IEEE Transactions on Vehicular Technology*, 71(10), 10280–10292. <https://doi.org/10.1109/TVT.2022.3184043>
- Wang, W. F., Balkcom, D., & Chakrabarti, A. (2015). A fast online spanner for roadmap construction. *International Journal of Robotics Research*, 34(11), 1418–1432. <https://doi.org/10.1177/0278364915576491>
- Wang, X., Pan, J. S., Yang, Q. Y., Kong, L. P., Snásel, V., & Chu, S. C. (2022). Modified Mayfly Algorithm for UAV Path Planning. *Drones*, 6(5), 134. <https://doi.org/10.3390/drones6050134>
- Wu, G. H., Shen, X., Li, H. F., Chen, H. K., Lin, A. P., & Suganthan, P. N. (2018). Ensemble of differential evolution variants. *Information Sciences*, 423, 172–186. <https://doi.org/10.1016/j.ins.2017.09.053>
- Wu, H. S., & Xiao, R. B. (2020). Flexible Wolf Pack Algorithm for Dynamic Multidimensional Knapsack Problems. *Research*, 2020, Article 1762107. <https://doi.org/10.34133/2020/1762107>
- Wu, H. S., Xue, J. J., Xiao, R. B., & Hu, J. Q. (2020). Uncertain bilevel knapsack problem based on an improved binary wolf pack algorithm. *Frontiers of Information Technology & Electronic Engineering*, 21(9), 1356–1368. <https://doi.org/10.1631/FITEE.1900437>
- Wu, H. S., & Zhang, F. M. (2014). Wolf Pack Algorithm for Unconstrained Global Optimization. *Mathematical Problems in Engineering*, 2014, Article 465082. <https://doi.org/10.1155/2014/465082>
- Wu, J. S., Li, R. H., Li, J. W., Zou, M. C., & Huang, Z. J. (2023). Cooperative unmanned surface vehicles and unmanned aerial vehicles platform as a tool for coastal monitoring activities. *Ocean & Coastal Management*, 232, Article 106421. <https://doi.org/10.1016/j.ocecoaman.2022.106421>
- Wu, Z. P., Meng, Z. J., Zhao, W. L., & Wu, Z. (2021). Fast-RRT: A RRT-Based Optimal Path Finding Method. *Applied Sciences-Basel*, 11(24), Article 11777. <https://doi.org/10.3390/app12141177>
- Xie, D. M., Hu, R. F., Wang, C. S., Zhu, C. H., Xu, H., & Li, Q. P. (2023). A Simulation Framework of Unmanned Aerial Vehicles Route Planning Design and Validation for Landslide Monitoring. *Remote Sensing*, 15(24), 5758. <https://doi.org/10.3390/rs15245758>
- Xing, L. D., & Johnson, B. W. (2023). Reliability theory and practice for unmanned aerial vehicles. *IEEE Internet of Things Journal*, 10(4), 3548–3566. <https://doi.org/10.1109/JIOT.2022.3218491>
- Xiu-Wu, Y. U., Hao, Y. U., Yong, L., & Ren-Rong, X. (2020). A clustering routing algorithm based on wolf pack algorithm for heterogeneous wireless sensor networks. *Computer Networks*, 167, Article 106994. <https://doi.org/10.1016/j.comnet.2019.106994>
- Xu, Y., Guan, G. F., Song, Q. W., Jiang, C., & Wang, L. H. (2020). Heuristic and random search algorithm in optimization of route planning for Robot's geomagnetic navigation. *Computer Communications*, 154, 12–17. <https://doi.org/10.1016/j.comcom.2020.02.043>
- Xu, Z. N., Zhang, L., Ma, X. S., Liu, Y., Yang, L., & Yang, F. (2022). An Anti-Disturbance Resilience Enhanced Algorithm for UAV 3D Route Planning. *Sensors*, 22(6), 2151. <https://doi.org/10.3390/s22062151>
- Yao, W. R., Chen, Y., Fu, J. Y., Qu, D., Wu, C. W., Liu, J. X., Sun, G. H., & Xin, L. M. (2023). Evolutionary Utility Prediction Matrix-Based Mission Planning for Unmanned Aerial Vehicles in Complex Urban Environments. *IEEE Transactions on Intelligent Vehicles*, 8(2), 1068–1080. <https://doi.org/10.1109/TIV.2022.3192525>
- Yildiz, B., Aslan, M. F., Durdu, A., & Kayabasi, A. (2024). Consensus-based virtual leader tracking swarm algorithm with GDRRT*-PSO for path-planning of multiple-UAVs. *Swarm and Evolutionary Computation*, 88, Article 101612. <https://doi.org/10.1016/j.swevo.2024.101612>
- Yu, X. B., & Luo, W. G. (2023). Reinforcement learning-based multi-strategy cuckoo search algorithm for 3D UAV path planning. *Expert Systems with Applications*, 223, Article 119910. <https://doi.org/10.1016/j.eswa.2023.119910>
- Zhang, Y. D., Jun, Y., Wei, G., & Wu, L. N. (2010). Find multi-objective paths in stochastic networks via chaotic immune PSO. *Expert Systems with Applications*, 37(3), 1911–1919. <https://doi.org/10.1016/j.eswa.2009.07.025>
- Zhang, Z., Jiang, J., Wu, J., & Zhu, X. Z. (2023). Efficient and optimal penetration path planning for stealth unmanned aerial vehicle using minimal radar cross-section tactics and modified A-Star algorithm. *ISA Transactions*, 134, 42–57. <https://doi.org/10.1016/j.isatra.2022.07.032>
- Zhou, W. H., Liu, Z. H., Li, J., Xu, X., & Shen, L. C. (2021). Multi-target tracking for unmanned aerial vehicle swarms using deep reinforcement learning. *Neurocomputing*, 466, 285–297. <https://doi.org/10.1016/j.neucom.2021.09.044>